Monomorphic epitheliotropic intestinal T-cell lymphoma comprises morphologic and genomic heterogeneity impacting outcome

Luis Veloza,[1*] Doriane Cavalieri,[2*] Edoardo Missiaglia,[1] Albane Ledoux-Pilon,[3] Bettina Bisig,[1] Bruno Pereira,[4] Christophe Bonnet,[5] Elsa Poullot,[6] Leticia Quintanilla-Martinez,[7] Romain Dubois,[8] Francisco Llamas-Gutierrez,[9] Céline Bossard,[10] Roland De Wind,[11] Fanny Drieux,[12] Juliette Fontaine,[13] Marie Parrens,[14] Jeremy Sandrini,[15] Virginie Fataccioli,[6,16] Marie-Hélène Delfau-Larue,[16,17] Adrien Daniel,[18] Faustine Lhomme,[19] Lauriane Clément-Filliatre,[20] François Lemonnier,[16,21] Anne Cairoli,[22] Pierre Morel,[23] Sylvie Glaisner,[24] Bertrand Joly,[25] Abderrazak El Yamani,[26] Kamel Laribi,[27] Emmanuel Bachy,[28] Reiner Siebert,[29] David Vallois,[1] Philippe Gaulard,[6,16#] Olivier Tournilhac[2#] and Laurence de Leval[1#]

[1]Institute of Pathology, Department of Laboratory Medicine and Pathology, Lausanne University Hospital and Lausanne University, Lausanne, Switzerland; [2]Department of Hematology, University Hospital of Clermont-Ferrand, EA7453 CIC1405, Université Clermont Auvergne, Clermont-Ferrand, France; [3]Department of Pathology, University Hospital of Clermont-Ferrand, Clermont-Ferrand, France; [4]Clinical Research Direction, University Hospital of Clermont-Ferrand, Clermont-Ferrand, France; [5]Department of Hematology, University Hospital Sart Tilman, Liège, Belgium; [6]AP-HP, Henri Mondor Hospital, Pathology Department, Créteil, France; [7]Institute of Pathology, University Hospital Tübingen, Eberhard Karls University of Tübingen, Tübingen, Germany; [8]Department of Pathology, University Hospital of Lille, Lille, France; [9]Department of Pathology, University Center Hospital, Rennes, France; [10]Department of Pathology, CHU de Nantes, Nantes, France; [11]Department of Pathology, Institute Jules Bordet, Bruxelles, Belgique; [12]Service of Anatomical and Cytological Pathology, Center Henri Becquerel, Rouen, France; [13]Multisite Pathology Institute, Hôpital Lyon Sud, Hospices Civils de Lyon, Pierre Bénite, France; [14]Department of Pathology, CHU de Bordeaux, University of Bordeaux, Bordeaux, France; [15]Department of Pathology, Le Mans Hospital Center, Le Mans, France; [16]University Paris Est Créteil, INSERM, IMRB, Créteil, France; [17]Department of Immunobiology and INSERM U955, Henri Mondor University Hospital, Créteil, France; [18]Department of Hematology, University Hospital of Lille, Lille, France; [19]Department of Hematology, University Hospital of Rennes, Hospital Pontchaillou, Rennes, France; [20]Department of Oncology, Louis Pasteur Clinic, Essey-Lès-Nancy, France; [21]AP-HP, Henri Mondor Hospital, Lymphoid Malignancies Unit, Créteil, France; [22]Service of Hematology, Department of Oncology, Lausanne University, Hospital and Lausanne University, Lausanne, Switzerland; [23]Department of Hematology, Hospital of Lens, Lens and Department of Hematology, University Hospital of Amiens, Amiens, France; [24]Department of Hematology, Institute Curie, Hospital Rene Huguenin, Saint-Cloud, France; [25]Department of Hematology, Sud-Francilien Hospital Center, Corbeil-Essonnes, France; [26]Department of Hematology, Hospital Center of Blois, Blois, France; [27]Department of Hematology, Hospital Center Le Mans, Le Mans, France; [28]Department of Hematology, Center Hospitalier Lyon Sud and INSERM U1111, Pierre Bénite, France and [29]Institute of Human Genetics, Ulm University and Ulm University Medical Center, Ulm, Germany

[*]LV and DC contributed equally as co-first authors.
[#]PG, OT and LdL contributed equally as co-senior authors.

Correspondence: L. de Leval
Laurence.deleval@chuv.ch

Received: April 12, 2022.
Accepted: June 9, 2022.
Prepublished: June 16, 2022.

https://doi.org/10.3324/haematol.2022.281226

Supplementary material

Veloza L, Cavalieri D et al.

Monomorphic epitheliotropic Intestinal T-cell lymphoma comprises morphologic and genomic heterogeneity impacting outcome

Supplementary methods

Histology, immunohistochemistry, and FISH

All cases were reviewed, and diagnoses confirmed by the senior pathologists (LdL or PG). The tissues analysed comprised 68 gastrointestinal tumors, one omental mass and two abdominal lymph nodes. The latter three patients had clinical evidence of gastrointestinal involvement. The samples mostly consisted of surgical resections (n=62), or endoscopic or surgical biopsies (n=9). Sixty-three gastrointestinal samples were from the small intestine (12: ileum, 13: jejunum, 5: duodenum, unspecified 33); 3 were from the colon, and one each anal and gastric.

Immunohistochemistry was performed on 4 µm FFPE sections using specific antibodies (**Supplementary Table S1**) on automated immunostainers (BenchMark XT and Ultra; Ventana Medical Systems, Tucson, AZ). For the subset of cases previously published SETD2, H3K36me3 and H3K36me2 immunostainings had been performed manually[1].

Immunostainings were evaluated by eye-balling by estimating of the extent (<5%, 5-25%, 26-50%, 51-75%, 76-100%) and intensity (weak, moderate, strong) of the staining. Negative staining with no internal positive controls were considered non-contributive. In general, a threshold of 5% positivity extent was considered for positive score. For Ki-67, MYC and p53, staining were scored by quartiles (<25%, 26-50%, 51-75%, 76-100%). MYC was considered overexpressed when ≥ 25% of cells showed nuclear expression with moderate/strong intensity while a tumor was defined as *"p53* mutation pattern" positive when ≥ 50% of cells showed strong expression or when a complete lack of staining was observed. A high proliferation was defined as a Ki-67 immunostaining ≥ 50%. For SETD2, H3K36me3 and H3K36me2, immunostainings were scored (0 to 12) by multiplying extent (<10%: 0, 10-25%:1, 26-50%:2, 51-75%:3, 76-100%:5) and intensity (weak:1, moderate:2,

strong:3) of the staining as previously published[1]. Defective trimethylation was defined by H3K36me3 /H3K36me2 scores ratio < 1 and/or an H3K36me3 or SETD2 scores ≤ 6. Annotations and scorings were validated independently by two observers; discordant results were resolved by consensus with senior pathologists.

Chromogenic in situ hybridization for the detection of Epstein-Barr virus (EBV) was performed with EBV–encoded RNA (EBER) probes (INFORM, EBER Probe; Ventana Medical Systems), according to the manufacturer's recommendations, with an automated slide stainer (BenchMark XT; Ventana Medical Systems).

FISH labelling was performed using the ZytoLight FISH-Tissue Implementation Kit (ZytoVision, Bremerhaven, Germany) according to the manufacturer's protocol, with a minor modification (digestion with pepsin was performed for 13 min at 37°C). Subsequent steps of FISH labelling were carried out as previously described[1]. Labelled slides were analysed with a Zeiss AxioImager Z2 fluorescence microscope (Carl Zeiss, Oberkochen, Germany) equipped with specific filters for FITC, SpectrumOrange, DAPI, and double and triple band-pass filters. Hybridization signals were examined with a Plan-APOCHROMAT 63x oil immersion objective (Carl Zeiss). Images were captured using ISIS digital image analysis system version 5.5 (Metasystems, Altlussheim, Germany).

For evaluation of the *SETD2* locus, as previously described[1], we used a bacterial artificial chromosome (BAC) probe overlapping with the 3' end of the *SETD2* locus (target probe at 3p21.31: RP11-425J9, GenBank reference AC094020.2) labelled with orange, and two BAC clones hybridizing to the 3p25 region (control probe at 3p25: RP11-266J6 and RP11-485N3, GenBank references AC011610.11/AC022382.4 and AQ633871.1/AQ633873.1, respectively), labelled with green. At least 50 tumor nuclei were analysed for each case, and > 11.2% of nuclei with a ratio of orange to green signals ≤ 0.5 was considered indicative of *SETD2* deletion.

To detect *MYC* alterations, a commercial LSI *MYC* Dual Color Break Apart Rearrangement Probe (8q24) was used (Abbott Molecular, Des Plaines, IL, USA), and at least 50 nuclei were evaluated for each case. Cases were classified into *MYC* copy gain-positive if the average number of *MYC* copies per nucleus was ≥ 3. In case of *MYC* copy gain, the 3p25 control probe (used for *SETD2* locus evaluation, see above) was used to exclude a possible hyperploidy; the latter was considered in case of a concomitant *MYC* and 3p25 copy gain (average copies ≥ 3). *MYC* rearrangement was defined by > 10% of nuclei with split signals.

DNA isolation

Genomic DNA (gDNA) was extracted from unstained FFPE sections. Areas with highest tumor cell content and those devoid of neoplastic cells were marked on HE slides by a pathologist and subsequently reported on corresponding FFPE sections stained with toluidine blue. Manual microdissection of the regions of interest was performed under a microscope, followed by genomic DNA extraction using Maxwell® 16 Plus LEV DNA FFPE Purification Kit (Promega), according to the manufacturer's instructions. gDNAs were quantified by Qubit fluorometer (Thermo Fisher Scientific), and their quality and size distribution were assessed by capillary electrophoresis using Fragment Analyzer with High Sensitivity Genomic DNA Analysis Kit, following manufacturer's instructions.

Whole exome sequencing (WES)

Thirty-four cases were analyzed by WES, including, 14 previously reported[1]. For the remaining 20 samples, 500 ng of paired tumoral and normal DNA were sheared with Covaris S220 using AFA 520045 tubes and the following settings: duty Factor 10%; Peak Incident Power 175; Cycle/Busrt 200 and time 3 or 5 minutes depending on DNA quality. Libraries were performed using the Kapa Hyperplus library preparation kit (Roche,

Pleasanton, CA) combined to the xgen research panel v1.0 and UMIs (in order to identify PCR duplicates) from IDT DNA (Newark, New Jersey, USA). Captures were pooled further and paired-end sequenced on a HiSeq 4000 from Illumina (San Diego, CA). On average, around 80 million pair-end reads per sample were sequenced reaching a mean coverage of 204X (range 132-381) for tumor and 200X (range 115-380) for normals.

Targeted deep sequencing (TDS)

34 samples were subject to TDS using a customized panel covering 27 genes relevant to T-cell lymphoma biology (*ARID1A, ATM, BCOR, CARD11, CCR4, CD28, CTNNB1, DDX3X, DNMT3A, FYN, IDH2, IRF4, JAK1, JAK3, KMT2D, PIK3CD, PLCG1, PRKCB, RHOA, SETD2, SOCS1, STAT3, STAT5B, TET2, TNFRSF1B, TP53, VAV1*). Briefly, 100 to 200 ng of gDNA template was used to prepare DNA libraries with the KAPA HyperPlus library preparation kit (Roche, Pleasanton, CA). Target enrichment of the DNA libraries was performed by hybridization capture with a custom design of xGen Lockdown Probes (Integrated DNA Technologies, Coralville, IA) covering the full coding sequences of the targeted genes. Enriched libraries were sequenced on a MiSeq™ equipment (Illumina) as previously described[2]. On average, we sequenced around 2.5 million pair-end reads per sample reaching a mean coverage of 1858X (range 129-3491).

Sequence analysis

Sequence analysis was based on established algorithms and pipelines according to GATK best practices (The Genome Analysis Toolkit) standards (Best practice variant detection with the GATK v.4.1, for release 2.0). Initial QC steps involved demultiplexing, quality assessment of the produced reads and adapter removal. Forward and reverse reads were aligned to the human genome (GATK repository, build 37 decoy) using BWA-MEM (v0.7.10) [2]. BAM files were subjected to PCR duplicate removal using Unique Molecular

Indexes (fgbio v0.6.1) (WES analysis) or MarkDuplicates (Picard – for TDS analysis), followed by realignment around indels (GATK tools v3.7) and base recalibration using (GATK tools v4.1).

For WES analysis, the variant call was restricted to the 27 genes included in the TDS panel plus the *GNAI2* gene. Single nucleotide and indel variant calling was performed using VarScan (v2.4.4) and MuTect2 algorithm (GATK v4.1) comparing tumor *versus* matched normal. Specifically for VarScan, reads from normal and tumor samples were pileup using samtools mpileup (v1.9) with the following parameters: -x (disable read-pair overlap detection), -B (disable per-base alignment quality), -d 1000000 (max depth), -q 1 (skip alignment with mapQ smaller than 1), -C 50 (adjust mapping quality), -m 3 (min number gapped reads for indels candidates) and -F 0.0002 (min fraction of gapped reads). The tumor and normal pileup files were compared by VarScan somatic algorithm using the following parameters: minimum variant allele frequency threshold=0.01, tumor purity (tumor dependent), normal purity=0.95, minimum read depth at a position to make a call=10 and Somatic p-value=0.1 (Fisher's Exact Test). Variants were further filtered employing bam-readcount (-q 1, -b 20) and fpfilter algorithm in VarScan.

For MuTect, a set of 46 normal samples was used to generate a Pool of Normal (PON), which was applied into the tumor/normal comparison. Call was performed using defaults parameters, but keeping the option “genotype-pon-site” as true.

Variants were further filtered using the FilterMutectCalls algorithm as described in https://github.com/broadinstitute/gatk/blob/master/docs/mutect/mutect.pdf.

Calls from the two callers were combined in R, considering the union of the VarScan and MuTect callers.

Further variant filtering was carried out using the following formula: VAF Norm<15% & VAF Tum>=40% & Cov.REF Norm >=18 reads & Cov.ALT Tum>5 reads & (VAF Tum- VAF Norm)>=30% OR VAF Norm<10% & VAF Tum<=40% & VAF Tum>5% & Cov.REF Norm >=18 reads & Cov.ALT Tum>5 reads & (VAF Tum- VAF Norm)>=5%, where VAF Norm and VAF Tum represent the allele frequencies observed for the variant in normal and tumor, respectively; Cov.REF and Cov.ALT represent the local coverage observed for the reference or the alternative sequence, respectively. Variants with a “PASS” in the caller filter were also retained, while they were excluded if part of the false positive genes reported by Fajardo et al.[3] or if described to be a polymorphism with MAF (minimum allele frequency) of 1% in the 1000Genome project (v.Oct2014), NIH-Exome Sequencing Project (ESP6500 - European ancestry subset) or ExAC (r.1).

For TDS analysis, single nucleotide and indel variant calling was performed using VarScan (v2.4.3) and MuTect2 algorithm (GATK v3.7). Specifically for VarScan, reads from tumor sample were pileup using samtools mpileup (v1.3) with the following parameters: -x (disable read-pair overlap detection), -B (disable per-base alignment quality), -d 1000000 (max depth), -q 1 (skip alignment with mapQ smaller than 1), -C 50 (adjust mapping quality), -m 3 (min number gapped reads for indels candidates) and -F 0.0002 (min fraction of gapped reads). The tumor pileup file was further analyzed with VarScan mpileup2snp and mpileup2indel functions using the following parameters: minimum variant allele frequency threshold=0.01, minimum average quality 20, minimum coverage of 50 reads, minimum read depth at a position to make a call=10 and Somatic p-value=0.1 (Fisher's Exact Test).

For MuTect, call was performed using defaults parameters. The union of the variants called by VarScan and MuTect were combined in R and filter using the following parameters: local coverage above 50 reads, at least 10 reads supporting the variant and allele

frequency above 1%. Variants were further filter using an internal list of artefacts developed during the development and validation of the TDS panel. Furthermore, considering the potential presence of germinal variants, mutations were also filtered if present in the gnomAD database with more than 9 alleles in any populations (excluding Ashkenazi), when tumor allele frequency was above 40%.

All variants were finally annotated for presence in dbSNP, the ExAC (r.1) and COSMIC (v88) databases as well as mutation effect on gene transcript by SnpEff (v.4.3t). Only nonsynonymous variants or alterations occurring in the splice-sites (last 2 nucleotides of the exon and the first 10 nucleotides of the introns) were retain in the final table.

All retained alterations were confirmed by visual inspection with the Integrative Genomics Viewer (IGV) tool.

It should be noted that 24 samples were analyzed with both WES and TDS panel, showing complete agreement between the two analyses.

Statistical methods (extended)

The χ^2 test or Fisher's exact tests were used to determine associations between morphological, immunophenotypical and genetic characteristics of MEITL tumors. Estimates of overall survival were constructed using the Kaplan-Meier method. Cox proportional hazards regression model was used to investigate associated prognostic factors in univariate and multivariable analysis. The proportional-hazard hypothesis was verified using Schoenfeld's test and plotting residuals.

For multivariable analysis, the covariates were determined according to univariate results ($P \leq 0.10$) and to the clinical and biological relevance, restricted to available pretherapeutic features. A particular attention was paid on the multicolinearity and on the rules-of-thumb suggested for determining the minimum number of subjects required to conduct multiple

regression. Recommendations for sample size are heterogeneous and often with minimal empirical evidence. This is problematic because statistical procedures that create optimized combinations of variables tend to overfit the data. Thus, this overfitting can result in erroneous conclusions if models fit to one data set are applied to others.

Accordingly, the final multivariable model was built step by step, first focusing only on biological parameters (i) studying the relationships between the following covariables and (ii) evaluating the impact to add or delete them on multivariable analyses: B-cell marker expression, *TP53* mutation, *STAT5B* mutation, MYC expression (> 25%) and atypical histology). Following this step, atypical histology was excluded from multivariable analyses according to the significant relationship with *TP53* mutation, MYC expression.

The testing and parameter estimation performed using a statistical model clearly depends on the variables included in the model, it is therefore crucial for confounding adjustment that known clinically significant variables are included in the regression model. A clinically significant variable may well be an important confounder also when it is statistically insignificant. Then, clinical variables were included in multivariable analyses in addition to biological variables: performance status ≥2, age ≥70 and Lugano stage ≥2. Age and Lugano were not statistically significant. In final model, only performance status was retained with biological parameters.

The Akaike information criterion and Bayesian information criterion were calculated and used as model diagnostics to determine how well the model fit improved following addition of covariates. Results were expressed as hazard-ratio (HR) and 95% confidence interval.

Furthermore, to ensure the robustness of our results, the final model was validated by a two-step bootstrapping process. In each step, 1,000 bootstrap samples with replacements were created from the training set. In the first one, using the stepwise procedure, we determined the percentage of models including each of the initial variables. In the second step, we independently estimated the Cox model parameters of the final model. The

bootstrap estimates of each covariate coefficient and standard errors were averaged from those replicates.

A sensitivity analysis, including also age ≥70 and Lugano stage ≥2 in addition to aforementioned covariables (performance status and biological variables), was conducted. Statistical analysis was performed using Stata software (version 15, StataCorp LP, College Station, US). The tests were two-sided, with a type I error set at 5%. When appropriate, a correction of the type I error was applied to take into account multiple comparisons: Bonferroni method for the relationships between morphological, immunophenotypical and genetic characteristics of MEITL tumors and Sidak method for two by two multiple comparisons concerning overall survival.

Supplementary tables

Supplementary Table S1. List of antibodies used for immunohistochemical studies

Antibody	Clone	Source	Dilution
CD3	2GV6	Ventana Medical Systems, Tucson, AZ	RTU
CD20	L26	Novocastra, Newcastle, UK	1/400
CD2	AB75	Novocastra, Newcastle, UK	1/30
CD4	SP35	Ventana Medical Systems, Tucson, AZ	RTU
CD5	SP19	Abcam, Cambridge, UK	1/40
CD7	CBC.37	DakoCytomation; Agilent Technologies, Santa Clara, CA	1/25
CD8	C8/144B	DakoCytomation; Agilent Technologies, Santa Clara, CA	1/30
CD30	Ber-H2	DakoCytomation; Agilent Technologies, Santa Clara, CA	1/30
CD56	CD564	Novocastra, Newcastle, UK	1/25
CD79a	JCB117	DakoCytomation; Agilent Technologies, Santa Clara, CA	1/50
CD103	EPR4166	GeneTex, Irvine, CA	1/300
TIA-1	2G9A10F5	Beckman Coulter, Brea, CA	1/1000
Granzyme B	GrB-7	Monosan, Uden, The Netherlands	1/30
Perforin	5B10	Diagnostic Biosystem, Pleasanton, CA	1/10
PD1	NAT105	Ventana Medical Systems, Tucson, AZ	RTU
Ki-67	MIB-1	DakoCytomation, Agilent Technologies, Santa Clara, CA	1/50
TCRb-F1	8A3	Thermo Fisher Scientific, Waltham, MA	1/30
TCRγ	3.20	Thermo Fisher Scientific, Waltham, MA	1/100
TCRδ	H41	Santa Cruz, Dallas, TX	1/200
SETD2	Polyclonal	Sigma, Sigma-Aldrich, St. Louis, MO	1/200
H3K36me3	Polyclonal	Abcam, Cambridge, UK	1/200
H3K36me2	Polyclonal	Abcam, Cambridge, UK	1/250
PAX5	SP34	Ventana Medical Systems, Tucson, AZ	RTU
MYC	Y69	Ventana Medical Systems, Tucson, AZ	RTU
P53	DO-7	DakoCytomation, Agilent Technologies, Santa Clara, CA	1/500

Abbreviation: RTU, ready-to-use

Supplementary Table S2. Localizations and extension of MEITL tumors

GI tract involvement	100%	63/63
Small bowel only	73.0%	46/63
Small bowel + large bowel	17.5%	11/63
Small bowel + stomach	1.6%	1/63
Small bowel + no extension data*	4.8%	3/63
Large bowel only	1.6%	1/63
Anus only	1.7%	1/63
Small bowel involvement		
Duodenum only	6.6%	4/61
Jejunum only	23.0%	14/61
Ileum only	24.6%	15/61
Multi-site involvement	6.6%	4/61
Not specified	39.3%	24/61
Lymph node involvement**		
Infradiaphragmatic	48.3%	29/60
Supradiaphragmatic	16.7%	10/60
Both	10%	6/60
Extranodal/extraGI involvement**	31.7%	19/60
Lung	8.3%	5/60
Liver	6.7%	4/60
Pleura	5%	3/60
Bone marrow***	7.4%	2/27
Abdominal wall	3.3%	2/60
Pelvis	3.3%	2/60
Bladder	3.3%	2/60
Other sites****	8.3%	5/60

*In 3 patients a small bowel involvement was documented, but not data available for other gastrointestinal sites (CT/PET/surgery report). **In 3 patients, no extension data were available regarding lymph node extension and extranodal involvement. ***Only 27 patients had a bone marrow biopsy at diagnosis. **** Other sites included pancreas (n=1), kidney (n=1), spleen (n=1), testis (n=1), and sphenoïd sinus (n=1).

Supplementary Table S3. Biological findings in MEITL patients at diagnosis

Protein C reactive		
Normal	12.1%	5/41
05-50	24.4%	10/41
>50	63.4%	26/41
Kidney failure	17%	8/47
Elevated liver enzymes	9.5%	4/42
Hypercalcemia	2.5%	1/40
CSF involvement	0%	0/13
Positive coeliac serology*	0%	0/18

Abbreviation: CSF, cerebrospinal fluid involvement.

*Coeliac serology included screening for anti-endomysium, anti-transglutaminase and/or anti-gliadin antibodies.

Supplementary Table S4. Correlations between morphological, immunophenotypical and genetic characteristics of MEITL tumors

	Necrosis	Angiotropism/ angioinvasion	Starry-sky/apoptosis	Non-monomorphic	Atypical histology	Epitheliotropism	CD56+	CD8+	B-cell antigen expression	Activated cytotoxic+	CD103+	TCRγδ+TCRβ- (vs TCRγδ-TCRβ+)	KI-67 >50%	p53 mutated pattern IHC	*TP53* mutation	MYC IHQ >25%	*MYC* gene alteration	*STAT5B* mutation
Angiotropism/angioinvasion	0.09																	
Starry-sky/apoptosis	1	0.38																
Non-monomorphic	0.26	0.04	0.08															
Atypical histology	0.004	<0.001	0.02	<0.001														
Epitheliotropism	0.48	0.95	0.78	0.18	0.56													
CD56+	0.76	0.97	0.93	0.32	0.56	0.93												
CD8+	1	1	0.92	1	1	0.90	1											
B-cell antigen expression	0.76	1	1	1	1	1	1	0.76										
Activated cytotoxic +	0.94	0.95	1	1	0.97	0.93	1	0.65	0.58									
CD103+	0.95	1	0.76	1	0.92	1	0.76	1	0.97	0.95								
TCRγδ+TCRβ- (vs TCRγδ-TCRβ+)	1	0.97	1	0.97	1	0.92	1	0.73	0.97	0.26	1							
Ki-67 >50%	0.30	0.93	0.95	0.33	0.33	0.78	0.05	0.76	0.92	0.68	0.18	1						
P53 mutated pattern IHC	0.97	0.18	0.82	<0.001	0.01	0.11	0.95	0.95	0.92	0.48	1	1	0.61					
***TP53* mutation**	0.90	0.33	0.63	<0.001	0.02	0.35	0.52	0.76	0.92	0.66	1	0.92	0.56	<0.001				
MYC IHQ >25%	0.41	0.56	0.61	0.03	0.07	0.76	0.78	0.94	1	0.95	0.97	1	1	0.33	0.06			
***MYC* gene alteration**	0.78	0.90	0.95	0.35	0.76	0.35	0.59	0.70	0.78	0.76	0.95	1	0.35	0.13	0.05	<0.001		
***STAT5B* mutation**	0.33	1	0.48	1	0.95	0.78	0.56	1	0.48	0.97	0.06	0.92	0.73	0.56	0.33	1	1	
***JAK3* mutation**	0.90	0.93	1	0.93	1	0.95	0.76	0.76	1	0.90	0.59	0.76	0.01	1	1	0.93	0.76	0.48

Abbreviation: IHC, immunohistochemistry.

Red cell: positive correlation; blue cell: expected correlation (by definition)

The χ^2 test and Fisher's exact tests were used to determine associations between variables and groups. Two-sided $p<0.05$ were considered to be statistically significant. p-values were adjusted for multiple testing with Benjamini & Hochberg method.

Supplementary Table S5. List of mutations identified in MEITL patients by WES and targeted sequencing.

SampleID	Chrom.	Position	Ref	Alt	ExonicFunc.refGene	Cytoband	Gene Symbol	Reference ID	Results (HGVS.c, HGVS.p)	Allele Frequenc	Coverage	TDS‡	WES‡
MEITL-1	1	27101348	T	C	missense_variant	1p36	ARID1A	NM_006015.4	c.4630T>C (p.Ser1544Pro)	39.2%	199X	Nat Comm	Exome.Ag
MEITL-1	11	108121804	G	A	splice_donor_variant&splice_region_variant&intron_variant	11q22	ATM	NM_000051.3	c.1607+5G>A	40.23%	87X	Nat Comm	Exome.Ag
MEITL-1	17	7577532	G	A	missense_variant	17p13	TP53	NM_000546.5	c.749C>T (p.Pro250Leu)	44.44%	72X	Nat Comm	Exome.Ag
MEITL-1	3	50293695	G	A	missense_variant	3p21	GNAI2	NM_002070.3	c.536G>A (p.Arg179His)	34.92%	63X	Nat Comm	Exome.Ag
MEITL-1	3	50294174	C	A	missense_variant	3p21	GNAI2	NM_002070.3	c.613C>A (p.Gln205Lys)	35.48%	31X	Nat Comm	Exome.Ag
MEITL-1	X	39932851	GT	G	frameshift_variant	Xp11	BCOR	NM_001123383.1	c.1747del (p.Thr583Profs*6)	73.02%	63X	Nat Comm	Exome.Ag
MEITL-1	X	39933289	G	A	missense_variant	Xp11	BCOR	NM_001123383.1	c.1310C>T (p.Thr437Ile)	38.1%	168X	Nat Comm	Exome.Ag
MEITL-10	17	40359729	T	G	nonsynonymous SNV	17q21.2	STAT5B	NM_012448.3	c.1924A>C (p.Asn642His)	31.78%	815X	Nat Comm	none
MEITL-10	3	47162927	G	A	stopgain	3p21.31	SETD2	NM_014159.6	c.3199C>T (p.Gln1067*)	18.18%	1287X	Nat Comm	none
MEITL-11	17	40359659	T	A	missense_variant	17q21	STAT5B	NM_012448.3	c.1994A>T (p.Tyr665Phe)	42%	134X	NGSIyT	none
MEITL-11	X	39922118	C	T	missense_variant	Xp11	BCOR	NM_001123383.1	c.3952G>A (p.Asp1318Asn)	100%	86X	NGSIyT	none
MEITL-12	17	40354460	A	T	missense_variant	17q21	STAT5B	NM_012448.3	c.2135T>A (p.Val712Glu)	78.57%	14X	Nat Comm	Exome.Ag
MEITL-12	20	39794862	A	G	missense_variant	20q12	PLCG1	NM_002660.2	c.1828A>G (p.Ile610Val)	10.14%	217X	Nat Comm	Exome.Ag
MEITL-12	3	47143034	G	C	missense_variant	3p21	SETD2	NM_014159.6	c.4929C>G (p.Asn1643Lys)	82.76%	147X	Nat Comm	Exome.Ag
MEITL-14	19	17945912	G	C	missense_variant	19p13	JAK3	NM_000215.3	c.2027C>G (p.Pro676Arg)	54.94%	166X	Nat Comm	Exome.Ag
MEITL-14	19	17949108	C	T	missense_variant	19p13	JAK3	NM_000215.3	c.1533G>A (p.Met511Ile)	63.91%	135X	Nat Comm	Exome.Ag
MEITL-14	3	47147505	C	T	missense_variant	3p21	SETD2	NM_014159.6	c.4821G>A (p.Met1607Ile)	35.78%	563X	Nat Comm	Exome.Ag
MEITL-14	3	47161751	G	A	stop_gained	3p21	SETD2	NM_014159.6	c.4375C>T (p.Arg1459*)	47.18%	251X	Nat Comm	Exome.Ag
MEITL-15	17	40359729	T	G	missense_variant	17q21	STAT5B	NM_012448.3	c.1924A>C (p.Asn642His)	85.25%	62X	Nat Comm	Exome.Ag
MEITL-15	3	47147518	TGGATGT	T	disruptive_inframe_deletion	3p21	SETD2	NM_014159.6	c.4793_4807del (p.Arg1598_Ile1602del)	32%	227X	Nat Comm	Exome.Ag
MEITL-16	19	17948006	G	A	missense_variant	19p13	JAK3	NM_000215.3	c.1718C>T (p.Ala573Val)	35%	701X	NGSIyT	none
MEITL-16	19	17949121	T	G	missense_variant	19p13	JAK3	NM_000215.3	c.1520A>C (p.Gln507Pro)	42%	308X	NGSIyT	none
MEITL-16	3	47155365	C	A	splice_donor_variant&intron_variant	3p21	SETD2	NM_014159.6	c.4715+1G>T	30%	318X	NGSIyT	none
MEITL-16	3	47164495	G	T	stop_gained	3p21	SETD2	NM_014159.6	c.1631C>A (p.Ser544*)	19%	64X	NGSIyT	none
MEITL-17	1	65306942	G	A	missense_variant	1p31	JAK1	NM_002227.3	c.2635C>T (p.Arg879Cys)	10.93%	377X	Nat Comm	Exome.Ag
MEITL-17	17	40359729	T	G	missense_variant	17q21	STAT5B	NM_012448.3	c.1924A>C (p.Asn642His)	91.3%	70X	Nat Comm	Exome.Ag
MEITL-17	19	17945970	G	A	missense_variant	19p13	JAK3	NM_000215.3	c.1969C>T (p.Arg657Trp)	38.89%	91X	Nat Comm	Exome.Ag
MEITL-17	3	47058637	GTACT	G	frameshift_variant	3p21	SETD2	NM_014159.6	c.7637_7640del (p.Lys2546Thrfs*17)	32.67%	300X	Nat Comm	Exome.Ag
MEITL-17	3	47125468	AG	A	frameshift_variant	3p21	SETD2	NM_014159.6	c.5801del (p.Pro1934Leufs*11)	38.72%	359X	Nat Comm	Exome.Ag
MEITL-19	17	40359678	G	A	missense_variant	17q21	STAT5B	NM_012448.3	c.1975C>T (p.Arg659Cys)	2%	1482X	NGSIyT	none
MEITL-19	17	40359729	T	G	missense_variant	17q21	STAT5B	NM_012448.3	c.1924A>C (p.Asn642His)	26%	1302X	NGSIyT	none
MEITL-19	19	17948006	G	A	missense_variant	19p13	JAK3	NM_000215.3	c.1718C>T (p.Ala573Val)	4%	1122X	NGSIyT	none
MEITL-19	3	47059132	C	G	missense_variant	3p21	SETD2	NM_014159.6	c.7529G>C (p.Arg2510Pro)	55%	1025X	NGSIyT	none
MEITL-2	12	49441785	C	T	missense_variant	12q13	KMT2D	NM_003482.3	c.4199G>A (p.Cys1400Tyr)	42.05%	289X	Nat Comm	Exome.Ag
MEITL-2	17	7577538	C	T	missense_variant	17p13	TP53	NM_000546.5	c.743G>A (p.Arg248Gln)	91.47%	129X	Nat Comm	Exome.Ag
MEITL-2	3	47058746	T	G	splice_acceptor_variant&intron_variant	3p21	SETD2	NM_014159.6	c.7534-2A>C	40.82%	302X	Nat Comm	Exome.Ag
MEITL-2	3	47155483	C	T	missense_variant	3p21	SETD2	NM_014159.6	c.4598G>A (p.Cys1533Tyr)	41.98%	541X	Nat Comm	Exome.Ag
MEITL-20	17	40359729	T	G	missense_variant	17q21	STAT5B	NM_012448.3	c.1924A>C (p.Asn642His)	49.12%	116X	Nat Comm	Exome.Ag
MEITL-20	19	17948006	G	A	missense_variant	19p13	JAK3	NM_000215.3	c.1718C>T (p.Ala573Val)	51.72%	29X	Nat Comm	Exome.Ag
MEITL-20	3	47164398	TGTACAA	T	frameshift_variant	3p21	SETD2	NM_014159.6	c.1718_1727del (p.Phe573*)	40.51%	158X	Nat Comm	Exome.Ag
MEITL-20	3	47205343	C	T	splice_donor_variant&intron_variant	3p21	SETD2	NM_014159.6	c.71+1G>A	30.65%	63X	Nat Comm	Exome.Ag
MEITL-203	1	9780849	A	C	missense_variant	1p36	PIK3CD	NM_005026.3	c.1571A>C (p.Tyr524Ser)	32%	2011X	NGSIyT	none
MEITL-203	2	25462086	T	A	splice_acceptor_variant&intron_variant	2p23	DNMT3A	NM_022552.4	c.2323-2A>T	46%	1310X	NGSIyT	none
MEITL-203	3	47165110	A	C	stop_gained	3p21	SETD2	NM_014159.6	c.1016T>G (p.Leu339*)	34%	3978X	NGSIyT	none
MEITL-203	3	47165722	G	C	stop_gained	3p21	SETD2	NM_014159.6	c.404C>G (p.Ser135*)	31%	3570X	NGSIyT	none
MEITL-21	17	7578283	G	T	missense_variant	17p13	TP53	NM_000546.5	c.566C>A (p.Ala189Asp)	62.28%	294X	Nat Comm	Exome.Ag
MEITL-21	19	17948745	ATGCAGT	A	disruptive_inframe_deletion	19p13	JAK3	NM_000215.3	c.1688_1696del (p.Lys563_Cys565del)	24.4%	503X	Nat Comm	Exome.Ag
MEITL-21	3	47059204	A	C	missense_variant	3p21	SETD2	NM_014159.6	c.7457T>G (p.Leu2486Arg)	24.31%	144X	Nat Comm	Exome.Ag
MEITL-21	3	47098908	C	CCGGCTGTG	frameshift_variant	3p21	SETD2	NM_014159.6	c.6365_6366insTTGTGCCAGGACACAGCCG (p.	12.14%	384X	Nat Comm	Exome.Ag
MEITL-22	1	27089473	C	CCAGG	frameshift_variant	1p36	ARID1A	NM_006015.4	c.2433_2436dup (p.Pro813Alafs*5)	29.76%	84X	Nat Comm	Exome.Ag
MEITL-22	17	40354460	A	T	missense_variant	17q21	STAT5B	NM_012448.3	c.2135T>A (p.Val712Glu)	75.44%	57X	Nat Comm	Exome.Ag
MEITL-22	19	17949108	C	T	missense_variant	19p13	JAK3	NM_000215.3	c.1533G>A (p.Met511Ile)	27.78%	90X	Nat Comm	Exome.Ag
MEITL-22	3	47098913	G	GTTCTCCTTA	stop_gained&conservative_inframe_insertion	3p21	SETD2	NM_014159.6	c.6360_6361insTAAGGAGAA (p.Glu2120_Arg	21.88%	359X	Nat Comm	Exome.Ag
MEITL-22	3	47147591	A	T	missense_variant	3p21	SETD2	NM_014159.6	c.4735T>A (p.Tyr1579Asn)	32.37%	210X	Nat Comm	Exome.Ag

MEITL-23	17	40354787	T	A	nonsynonymous SNV	17q21.2	STAT5B	NM_012448.3	c.2117A>T (p.Gln706Leu)	95.61%	569X	Nat Comm	Exome.IDT
MEITL-23	19	17948006	G	A	missense_variant	19p13	JAK3	NM_000215.3	c.1718C>T (p.Ala573Val)	51.61%	155X	Nat Comm	Exome.IDT
MEITL-23	3	47058649	G	T	stopgain	3p21.31	SETD2	NM_014159.6	c.7629C>A (p.Tyr2543*)	75.41%	306X	Nat Comm	Exome.IDT
MEITL-23	3	47164727	T	A	stop_gained	3p21	SETD2	NM_014159.6	c.1399A>T (p.Lys467*)	21.54%	65X	Nat Comm	Exome.IDT
MEITL-24	17	40359729	T	G	missense_variant	17q21	STAT5B	NM_012448.3	c.1924A>C (p.Asn642His)	70.11%	87X	Nat Comm	Exome.Ag
MEITL-24	17	40359746	T	G	missense_variant&splice_region_variant	17q21	STAT5B	NM_012448.3	c.1907A>C (p.Gln636Pro)	60.94%	64X	Nat Comm	Exome.Ag
MEITL-24	17	7578530	A	G	missense_variant	17p13	TP53	NM_000546.5	c.400T>C (p.Phe134Leu)	79.22%	235X	Nat Comm	Exome.Ag
MEITL-24	3	47163203	C	A	stop_gained	3p21	SETD2	NM_014159.6	c.2923G>T (p.Gly975*)	28.76%	388X	Nat Comm	Exome.Ag
MEITL-24	X	41206209	AGAAAAC	A	conservative_inframe_deletion	Xp11	DDX3X	NM_001356.4	c.1717_1731del (p.Asn573_Glu577del)	56.03%	117X	Nat Comm	Exome.Ag
MEITL-24	X	41206236	C	G	stop_gained	Xp11	DDX3X	NM_001356.4	c.1740C>G (p.Tyr580*)	53.96%	139X	Nat Comm	Exome.Ag
MEITL-25	1	65307176	A	C	missense_variant	1p31	JAK1	NM_002227.3	c.2512T>G (p.Phe838Val)	43.05%	153X	Nat Comm	Exome.Ag
MEITL-25	17	40354460	A	T	missense_variant	17q21	STAT5B	NM_012448.3	c.2135T>A (p.Val712Glu)	81.82%	22X	Nat Comm	Exome.Ag
MEITL-25	3	47058649	G	C	stop_gained	3p21	SETD2	NM_014159.6	c.7629C>G (p.Tyr2543*)	40.59%	553X	Nat Comm	Exome.Ag
MEITL-25	3	47164536	AC	A	frameshift_variant	3p21	SETD2	NM_014159.6	c.1589del (p.Cys530Phefs*49)	41.52%	461X	Nat Comm	Exome.Ag
MEITL-26	17	40354787	T	A	missense_variant	17q21	STAT5B	NM_012448.3	c.2117A>T (p.Gln706Leu)	88.89%	73X	Nat Comm	Exome.Ag
MEITL-26	17	40362213	T	A	missense_variant	17q21	STAT5B	NM_012448.3	c.1882A>T (p.Thr628Ser)	93%	202X	Nat Comm	Exome.Ag
MEITL-26	3	47084126	G	GT	frameshift_variant	3p21	SETD2	NM_014159.6	c.7162dup (p.Thr2388Asnfs*41)	37.09%	304X	Nat Comm	Exome.Ag
MEITL-26	3	47144882	G	C	missense_variant	3p21	SETD2	NM_014159.6	c.4871C>G (p.Ser1624Cys)	47.3%	316X	Nat Comm	Exome.Ag
MEITL-27	19	17948006	G	A	missense_variant	19p13	JAK3	NM_000215.3	c.1718C>T (p.Ala573Val)	21%	281X	NGSIyT; Nat Comm	none
MEITL-27	20	39794862	A	G	missense_variant	20q12	PLCG1	NM_002660.2	c.1828A>G (p.Ile610Val)	22%	211X	NGSIyT; Nat Comm	none
MEITL-27	20	39802391	A	G	missense_variant	20q12	PLCG1	NM_002660.2	c.3494A>G (p.Asp1165Gly)	29%	86X	NGSIyT; Nat Comm	none
MEITL-27	3	47162268	A	C	stopgain	3p21.31	SETD2	NM_014159.6	c.3858T>G (p.Tyr1286*)	37.25%	102X	NGSIyT; Nat Comm	none
MEITL-28	17	40359729	T	G	missense_variant	17q21	STAT5B	NM_012448.3	c.1924A>C (p.Asn642His)	58.39%	149X	Nat Comm	Exome.IDT
MEITL-28	17	7577120	C	T	missense_variant	17p13	TP53	NM_000546.5	c.818G>A (p.Arg273His)	79.65%	231X	Nat Comm	Exome.IDT
MEITL-28	19	17948006	G	A	missense_variant	19p13	JAK3	NM_000215.3	c.1718C>T (p.Ala573Val)	50.72%	69X	Nat Comm	Exome.IDT
MEITL-3	3	47103835	TGCTAAG(	T	frameshift_variant&splice_acceptor_variant&splice_region_va	3p21	SETD2	NM_014159.6	c.6110-8_6110del (p.?)	16.14%	256X	Nat Comm	Exome.Ag
MEITL-3	X	39933279	TG	T	frameshift_variant	Xp11	BCOR	NM_001123383.1	c.1319del (p.Pro440Hisfs*2)	58.11%	224X	Nat Comm	Exome.Ag
MEITL-30	17	40354787	T	A	missense_variant	17q21	STAT5B	NM_012448.3	c.2117A>T (p.Gln706Leu)	72.9%	679X	NGSIyT; V1	Exome.IDT
MEITL-30	19	17945918	A	G	missense_variant	19p13	JAK3	NM_000215.3	c.2021T>C (p.Val674Ala)	35.98%	353X	NGSIyT; V1	Exome.IDT
MEITL-30	3	47129722	C	A	stop_gained	3p21	SETD2	NM_014159.6	c.5158G>T (p.Glu1720*)	47.42%	97X	NGSIyT; V1	Exome.IDT
MEITL-31	17	7578406	C	T	missense_variant	17p13	TP53	NM_000546.5	c.524G>A (p.Arg175His)	67.36%	144X	NGSIyT; V1	Exome.IDT
MEITL-31	19	17948006	G	A	missense_variant	19p13	JAK3	NM_000215.3	c.1718C>T (p.Ala573Val)	39.68%	126X	NGSIyT; V1	Exome.IDT
MEITL-31	3	47103828	G	A	stop_gained	3p21	SETD2	NM_014159.6	c.6118C>T (p.Arg2040*)	33.86%	127X	NGSIyT; V1	Exome.IDT
MEITL-33	17	40359729	T	G	missense_variant	17q21	STAT5B	NM_012448.3	c.1924A>C (p.Asn642His)	85%	565X	NGSIyT; V1	none
MEITL-33	2	20459167	G	A	missense_variant	2q33	CD28	NM_006139.3	c.376G>A (p.Glu126Lys)	43.6%	78X	NGSIyT; V1	none
MEITL-33	3	47165765	CA	C	frameshift_variant	3p21	SETD2	NM_014159.6	c.360del (p.Ile120Metfs*32)	80%	348X	NGSIyT; V1	none
MEITL-33	4	106156872	G	C	missense_variant	4q24	TET2	NM_001127208.2	c.1773G>C (p.Gln591His)	17.6%	255X	NGSIyT; V1	none
MEITL-34	1	9775768	G	A	missense_variant	1p36	PIK3CD	NM_005026.3	c.311G>A (p.Arg104His)	7.59%	79X	none	Exome.IDT
MEITL-34	1	9777666	C	A	missense_variant	1p36	PIK3CD	NM_005026.3	c.1002C>A (p.Asn334Lys)	12.4%	121X	none	Exome.IDT
MEITL-34	11	108175403	T	G	missense_variant&splice_region_variant	11q22	ATM	NM_000051.3	c.5498T>G (p.Val1833Gly)	28.09%	89X	none	Exome.IDT
MEITL-34	17	40359729	T	G	missense_variant	17q21	STAT5B	NM_012448.3	c.1924A>C (p.Asn642His)	80.66%	183X	none	Exome.IDT
MEITL-34	3	47058743	A	C	missense_variant&splice_region_variant	3p21	SETD2	NM_014159.6	c.7535T>G (p.Leu2512Arg)	37.93%	116X	none	Exome.IDT
MEITL-34	3	47162211	G	C	stop_gained	3p21	SETD2	NM_014159.6	c.3915C>G (p.Tyr1305*)	35.77%	137X	none	Exome.IDT
MEITL-35	19	17947967	A	T	missense_variant	19p13	JAK3	NM_000215.3	c.1757T>A (p.Leu586Gln)	36.24%	149X	none	Exome.IDT
MEITL-35	3	47084145	AG	A	frameshift_variant	3p21	SETD2	NM_014159.6	c.7143del (p.Ser2382Leufs*29)	33.48%	221X	none	Exome.IDT
MEITL-36	17	40359729	T	G	missense_variant	17q21	STAT5B	NM_012448.3	c.1924A>C (p.Asn642His)	90%	2396X	NGSIyT	none
MEITL-36	3	47161887	ACTCT	A	frameshift_variant	3p21	SETD2	NM_014159.6	c.4235_4238del (p.Glu1412Valfs*19)	39%	3583X	NGSIyT	none
MEITL-36	3	47165557	G	GGAGAT	frameshift_variant	3p21	SETD2	NM_014159.6	c.564_568dup (p.Pro190Hisfs*21)	38%	3816X	NGSIyT	none
MEITL-37	17	40359729	T	G	missense_variant	17q21	STAT5B	NM_012448.3	c.1924A>C (p.Asn642His)	96.88%	512X	V1	Exome.IDT
MEITL-37	17	7577539	G	A	missense_variant	17p13	TP53	NM_000546.5	c.742C>T (p.Arg248Trp)	86.73%	98X	V1	Exome.IDT
MEITL-37	19	17948006	G	A	missense_variant	19p13	JAK3	NM_000215.3	c.1718C>T (p.Ala573Val)	45%	100X	V1	Exome.IDT
MEITL-37	3	47127738	A	G	missense_variant	3p21	SETD2	NM_014159.6	c.5344T>C (p.Trp1782Arg)	97.04%	371X	V1	Exome.IDT
MEITL-37	3	50293704	C	T	missense_variant	3p21	GNAI2	NM_002070.3	c.545C>T (p.Thr182Ile)	40.48%	126X	V1	Exome.IDT
MEITL-38	1	65313304	C	A	missense_variant	1p31	JAK1	NM_002227.3	c.1810G>T (p.Asp604Tyr)	47.06%	204X	V1	Exome.IDT
MEITL-38	19	17948006	G	A	missense_variant	19p13	JAK3	NM_000215.3	c.1718C>T (p.Ala573Val)	90.91%	99X	V1	Exome.IDT
MEITL-38	3	47147591	A	T	missense_variant	3p21	SETD2	NM_014159.6	c.4735T>A (p.Tyr1579Asn)	93.94%	99X	V1	Exome.IDT
MEITL-39	17	40359729	T	G	missense_variant	17q21	STAT5B	NM_012448.3	c.1924A>C (p.Asn642His)	26.71%	161X	V1	Exome.IDT
MEITL-39	19	17948009	G	A	missense_variant	19p13	JAK3	NM_000215.3	c.1715C>T (p.Ala572Val)	69.84%	65X	V1	Exome.IDT
MEITL-39	3	47125871	A	T	missense_variant&splice_region_variant	3p21	SETD2	NM_014159.6	c.5399T>A (p.Ile1800Asn)	80.95%	42X	V1	Exome.IDT
MEITL-4	17	7578260	C	T	missense_variant	17p13	TP53	NM_000546.5	c.589G>A (p.Val197Met)	85.71%	126X	Nat Comm	Exome.Ag
MEITL-4	19	17948006	G	A	missense_variant	19p13	JAK3	NM_000215.3	c.1718C>T (p.Ala573Val)	54.17%	50X	Nat Comm	Exome.Ag
MEITL-4	3	47108557	T	A	splice_donor_variant&splice_region_variant&intron_variant	3p21	SETD2	NM_014159.6	c.6109+3A>T	85.37%	41X	Nat Comm	Exome.Ag
MEITL-40	17	40354460	A	T	missense_variant	17q21	STAT5B	NM_012448.3	c.2135T>A (p.Val712Glu)	77.4%	177X	V1	Exome.IDT
MEITL-40	17	40359746	T	C	missense_variant&splice_region_variant	17q21	STAT5B	NM_012448.3	c.1907A>G (p.Gln636Arg)	39.61%	154X	V1	Exome.IDT
MEITL-40	17	7577574	T	C	missense_variant	17p13	TP53	NM_000546.5	c.707A>G (p.Tyr236Cys)	72.13%	61X	V1	Exome.IDT
MEITL-40	3	47058661	TTTGTGTT	T	disruptive_inframe_deletion	3p21	SETD2	NM_014159.6	c.7604_7616delinsT (p.Asn2535_Lys2539deli	25%	192X	V1	Exome.IDT
MEITL-40	3	47155365	C	G	splice_donor_variant&intron_variant	3p21	SETD2	NM_014159.6	c.4715+1G>C	25.71%	140X	V1	Exome.IDT
MEITL-41	19	17948745	ATGCAGT	A	disruptive_inframe_deletion	19p13	JAK3	NM_000215.3	c.1688_1696del (p.Lys563_Cys565del)	7.88%	203X	V1	Exome.IDT
MEITL-41	3	47143034	G	C	missense_variant	3p21	SETD2	NM_014159.6	c.4929C>G (p.Asn1643Lys)	16.84%	95X	V1	Exome.IDT
MEITL-41	3	50293694	C	T	missense_variant	3p21	GNAI2	NM_002070.3	c.535C>T (p.Arg179Cys)	15.38%	78X	V1	Exome.IDT
MEITL-41	4	106157275	C	T	stop_gained	4q24	TET2	NM_001127208.2	c.2176C>T (p.Gln726*)	5.88%	255X	V1	Exome.IDT

MEITL-42	17	40359729	T	G	missense_variant	17q21	STAT5B	NM_012448.3	c.1924A>C (p.Asn642His)	100%	86X	none	Exome.IDT
MEITL-42	3	47058705	TAC	T	frameshift_variant	3p21	SETD2	NM_014159.6	c.7571_7572del (p.Cys2524*)	37.96%	108X	none	Exome.IDT
MEITL-42	3	47084050	C	A	splice_donor_variant&intron_variant	3p21	SETD2	NM_014159.6	c.7238+1G>T	36.21%	116X	none	Exome.IDT
MEITL-43	12	49420670	G	A	stop_gained	12q13	KMT2D	NM_003482.3	c.15079C>T (p.Arg5027*)	29%	2614X	NGSIyT	none
MEITL-43	17	40376874	G	A	missense_variant	17q21	STAT5B	NM_012448.3	c.298C>T (p.Arg100Cys)	17%	1524X	NGSIyT	none
MEITL-43	17	7577539	G	A	missense_variant	17p13	TP53	NM_000546.5	c.742C>T (p.Arg248Trp)	84%	1018X	NGSIyT	none
MEITL-43	19	17949108	C	T	missense_variant	19p13	JAK3	NM_000215.3	c.1533G>A (p.Met511Ile)	58%	2493X	NGSIyT	none
MEITL-43	3	47142943	C	A	splice_donor_variant&splice_region_variant&intron_variant	3p21	SETD2	NM_014159.6	c.5015+5G>T	43%	1169X	NGSIyT	none
MEITL-43	3	47162045	G	A	stop_gained	3p21	SETD2	NM_014159.6	c.4081C>T (p.Gln1361*)	39%	2221X	NGSIyT	none
MEITL-44	12	49431762	C	A	missense_variant	12q13	KMT2D	NM_003482.3	c.9377G>T (p.Gly3126Val)	49%	1756X	NGSIyT; V1	none
MEITL-44	16	24135155	G	A	splice_acceptor_variant&intron_variant	16p12	PRKCB	NM_002738.6	c.919-1G>A	36%	2340X	NGSIyT; V1	none
MEITL-44	3	47125235	A	G	missense_variant	3p21	SETD2	NM_014159.6	c.6035T>C (p.Leu2012Pro)	31%	2699X	NGSIyT; V1	none
MEITL-45	11	10820102[illegible]	T	C	missense_variant	11q22	ATM	NM_000051.3	c.7390T>C (p.Cys2464Arg)	49%	1405X	V2	none
MEITL-45	17	40359729	T	G	missense_variant	17q21	STAT5B	NM_012448.3	c.1924A>C (p.Asn642His)	42%	1396X	V2	none
MEITL-45	19	17949108	C	A	missense_variant	19p13	JAK3	NM_000215.3	c.1533G>T (p.Met511Ile)	34%	732X	V2	none
MEITL-45	20	39791914	G	T	missense_variant&splice_region_variant	20q12	PLCG1	NM_002660.2	c.788G>T (p.Gly263Val)	49%	524X	V2	none
MEITL-45	3	47163347	C	A	stop_gained	3p21	SETD2	NM_014159.6	c.2779G>T (p.Glu927*)	29%	1763X	V2	none
MEITL-45	7	2946316	C	T	missense_variant	7p22	CARD11	NM_032415.5	c.3421G>A (p.Glu1141Lys)	49%	553X	V2	none
MEITL-46	1	65325801	G	A	missense_variant	1p31	JAK1	NM_002227.3	c.1321C>T (p.His441Tyr)	38.56%	153X	NGSIyT	Exome.IDT
MEITL-46	19	17948006	G	A	missense_variant	19p13	JAK3	NM_000215.3	c.1718C>T (p.Ala573Val)	46.48%	71X	NGSIyT	Exome.IDT
MEITL-46	3	47127758	C	T	missense_variant	3p21	SETD2	NM_014159.6	c.5324G>A (p.Gly1775Glu)	10%	1646X	NGSIyT	Exome.IDT
MEITL-46	3	47142981	T	A	missense_variant	3p21	SETD2	NM_014159.6	c.4982A>T (p.Glu1661Val)	73.61%	72X	NGSIyT	Exome.IDT
MEITL-47	1	65305427	T	C	missense_variant	1p31	JAK1	NM_002227.3	c.2701A>G (p.Thr901Ala)	37%	1567X	NGSIyT	none
MEITL-47	19	17949108	C	G	missense_variant	19p13	JAK3	NM_000215.3	c.1533G>C (p.Met511Ile)	36%	1369X	NGSIyT	none
MEITL-47	3	47164596	A	T	stop_gained	3p21	SETD2	NM_014159.6	c.1530T>A (p.Tyr510*)	43%	1650X	NGSIyT	none
MEITL-47	3	47165661	T	TGG	frameshift_variant	3p21	SETD2	NM_014159.6	c.463_464dup (p.Leu156Hisfs*9)	36%	1771X	NGSIyT	none
MEITL-47	4	10618292[illegible]	CTG	C	frameshift_variant	4q24	TET2	NM_001127208.2	c.3965_3966del (p.Leu1322Argfs*16)	2%	1595X	NGSIyT	none
MEITL-49	11	10820227[illegible]	G	A	missense_variant	11q22	ATM	NM_000051.3	c.7618G>A (p.Val2540Ile)	50.54%	279X	none	Exome.IDT
MEITL-49	17	40354460	A	T	missense_variant	17q21	STAT5B	NM_012448.3	c.2135T>A (p.Val712Glu)	91.19%	227X	none	Exome.IDT
MEITL-49	17	7574017	C	A	missense_variant	17p13	TP53	NM_000546.5	c.1010G>T (p.Arg337Leu)	81%	100X	none	Exome.IDT
MEITL-49	19	17949108	C	T	missense_variant	19p13	JAK3	NM_000215.3	c.1533G>A (p.Met511Ile)	53.65%	274X	none	Exome.IDT
MEITL-49	2	25457290	C	T	splice_acceptor_variant&intron_variant	2p23	DNMT3A	NM_022552.4	c.2598-1G>A	41.15%	192X	none	Exome.IDT
MEITL-5	17	7578271	T	C	missense_variant	17p13	TP53	NM_000546.5	c.578A>G (p.His193Arg)	54%	337X	NGSIyT; Nat Comm	none
MEITL-5	3	47084145	A	AG	frameshift_variant	3p21	SETD2	NM_014159.6	c.7143dup (p.Ser2382Leufs*47)	35%	1528X	NGSIyT; Nat Comm	none
MEITL-5	3	47088067	A	AAT	frameshift_variant	3p21	SETD2	NM_014159.6	c.7006_7007dup (p.Thr2338Serfs*16)	30%	1654X	NGSIyT; Nat Comm	none
MEITL-50	19	17948745	ATGCAGT	A	disruptive_inframe_deletion	19p13	JAK3	NM_000215.3	c.1688_1696del (p.Lys563_Cys565del)	43.98%	166X	none	Exome.IDT
MEITL-50	3	47059132	C	G	missense_variant	3p21	SETD2	NM_014159.6	c.7529G>C (p.Arg2510Pro)	37.1%	62X	none	Exome.IDT
MEITL-50	3	47144849	C	A	missense_variant	3p21	SETD2	NM_014159.6	c.4904G>T (p.Cys1635Phe)	33.33%	101X	none	Exome.IDT
MEITL-51	19	17949121	T	G	missense_variant	19p13	JAK3	NM_000215.3	c.1520A>C (p.Gln507Pro)	30.36%	112X	none	Exome.IDT
MEITL-52	17	40359659	T	A	missense_variant	17q21	STAT5B	NM_012448.3	c.1994A>T (p.Tyr665Phe)	58.56%	333X	none	Exome.IDT
MEITL-52	19	17948006	G	A	missense_variant	19p13	JAK3	NM_000215.3	c.1718C>T (p.Ala573Val)	45.45%	77X	none	Exome.IDT
MEITL-52	3	47161913	T	A	stop_gained	3p21	SETD2	NM_014159.6	c.4213A>T (p.Lys1405*)	47.46%	118X	none	Exome.IDT
MEITL-53	17	40359729	T	G	missense_variant	17q21	STAT5B	NM_012448.3	c.1924A>C (p.Asn642His)	81.62%	185X	none	Exome.IDT
MEITL-53	19	17948006	G	A	missense_variant	19p13	JAK3	NM_000215.3	c.1718C>T (p.Ala573Val)	34.18%	79X	none	Exome.IDT
MEITL-53	3	47059133	G	C	missense_variant	3p21	SETD2	NM_014159.6	c.7528C>G (p.Arg2510Gly)	40.48%	126X	none	Exome.IDT
MEITL-53	3	47147534	G	A	stop_gained	3p21	SETD2	NM_014159.6	c.4792C>T (p.Arg1598*)	35.62%	146X	none	Exome.IDT
MEITL-54	17	40359729	T	G	missense_variant	17q21	STAT5B	NM_012448.3	c.1924A>C (p.Asn642His)	89.89%	178X	none	Exome.IDT
MEITL-54	3	47165608	A	T	stop_gained	3p21	SETD2	NM_014159.6	c.518T>A (p.Leu173*)	91.4%	221X	none	Exome.IDT
MEITL-55	17	7578402	GC	G	frameshift_variant	17p13	TP53	NM_000546.5	c.527del (p.Cys176Serfs*71)	81%	1444X	NGSIyT	none
MEITL-55	3	47155464	A	C	missense_variant	3p21	SETD2	NM_014159.6	c.4617T>G (p.Cys1539Trp)	43%	3881X	NGSIyT	none
MEITL-55	3	47165741	C	A	stop_gained	3p21	SETD2	NM_014159.6	c.385G>T (p.Glu129*)	44%	3783X	NGSIyT	none
MEITL-56	17	40359729	T	G	missense_variant	17q21	STAT5B	NM_012448.3	c.1924A>C (p.Asn642His)	83%	765X	NGSIyT	none
MEITL-56	17	7577538	C	T	missense_variant	17p13	TP53	NM_000546.5	c.743G>A (p.Arg248Gln)	81%	817X	NGSIyT	none
MEITL-56	3	47098304	TAGTTA	T	splice_donor_variant&splice_region_variant&intron_variant	3p21	SETD2	NM_014159.6	c.6963+2_6963+6del	16%	846X	NGSIyT	none
MEITL-56	3	47163533	TA	T	frameshift_variant	3p21	SETD2	NM_014159.6	c.2592del (p.Asn865Ilefs*26)	39%	1895X	NGSIyT	none
MEITL-57	17	7577526	A	G	missense_variant	17p13	TP53	NM_000546.5	c.755T>C (p.Leu252Pro)	66%	818X	NGSIyT	none
MEITL-57	19	17955108	C	T	missense_variant	19p13	JAK3	NM_000215.3	c.119G>A (p.Arg40His)	49%	2612X	NGSIyT	none
MEITL-57	3	47058734	C	CCTGTAGT	frameshift_variant	3p21	SETD2	NM_014159.6	c.7541_7543delinsCCGACTACAG (p.His2514P	47%	1984X	NGSIyT	none
MEITL-58	17	40359729	T	G	missense_variant	17q21	STAT5B	NM_012448.3	c.1924A>C (p.Asn642His)	47%	2059X	NGSIyT; V1	none
MEITL-58	19	17948006	G	A	missense_variant	19p13	JAK3	NM_000215.3	c.1718C>T (p.Ala573Val)	41%	1434X	NGSIyT; V1	none
MEITL-58	3	47165024	G	A	stop_gained	3p21	SETD2	NM_014159.6	c.1102C>T (p.Arg368*)	40%	3102X	NGSIyT; V1	none
MEITL-58	4	10619403[illegible]	C	T	missense_variant	4q24	TET2	NM_001127208.2	c.4492C>T (p.Arg1498Cys)	46%	2951X	NGSIyT; V1	none
MEITL-59	17	40364159	C	T	missense_variant	17q21	STAT5B	NM_012448.3	c.1523G>A (p.Cys508Tyr)	45%	2389X	NGSIyT	none
MEITL-59	17	7578406	C	T	missense_variant	17p13	TP53	NM_000546.5	c.524G>A (p.Arg175His)	49%	2011X	NGSIyT	none
MEITL-59	3	47098421	G	A	stop_gained	3p21	SETD2	NM_014159.6	c.6853C>T (p.Gln2285*)	28%	2839X	NGSIyT	none
MEITL-59	3	47125799	A	C	missense_variant	3p21	SETD2	NM_014159.6	c.5471T>G (p.Ile1824Ser)	13%	2665X	NGSIyT	none
MEITL-59	3	47165261	C	T	missense_variant	3p21	SETD2	NM_014159.6	c.865G>A (p.Asp289Asn)	5%	2588X	NGSIyT	none

MEITL-6	1	65309803	G	A	missense_variant	1p31	JAK1	NM_002227.3	c.2347C>T (p.Leu783Phe)	15.31%	522X	Nat Comm	Exome.IDT
MEITL-6	1	65312365	A	G	missense_variant	1p31	JAK1	NM_002227.3	c.1954T>C (p.Tyr652His)	8.97%	301X	Nat Comm	Exome.IDT
MEITL-6	17	7579362	A	C	missense_variant	17p13	TP53	NM_000546.5	c.325T>G (p.Phe109Val)	87.54%	321X	Nat Comm	Exome.IDT
MEITL-6	19	17949108	C	T	missense_variant	19p13	JAK3	NM_000215.3	c.1533G>A (p.Met511Ile)	55.73%	314X	Nat Comm	Exome.IDT
MEITL-62	17	7577121	G	A	missense_variant	17p13	TP53	NM_000546.5	c.817C>T (p.Arg273Cys)	19%	1898X	NGSlyT	none
MEITL-62	17	7579356	G	T	missense_variant	17p13	TP53	NM_000546.5	c.331C>A (p.Leu111Met)	22%	1672X	NGSlyT	none
MEITL-62	19	17947968	G	C	missense_variant	19p13	JAK3	NM_000215.3	c.1756C>G (p.Leu586Val)	27%	1126X	NGSlyT	none
MEITL-62	3	47098450	G	C	stop_gained	3p21	SETD2	NM_014159.6	c.6824C>G (p.Ser2275*)	21%	3483X	NGSlyT	none
MEITL-63	1	65305421	C	T	missense_variant	1p31	JAK1	NM_002227.3	c.2707G>A (p.Glu903Lys)	40%	2717X	NGSlyT	none
MEITL-63	17	7577547	C	T	missense_variant	17p13	TP53	NM_000546.5	c.734G>A (p.Gly245Asp)	82%	911X	NGSlyT	none
MEITL-63	19	17949121	T	G	missense_variant	19p13	JAK3	NM_000215.3	c.1520A>C (p.Gln507Pro)	85%	2760X	NGSlyT	none
MEITL-63	3	47098937	G	GGC	frameshift_variant	3p21	SETD2	NM_014159.6	c.6336_6337insGC (p.Arg2113Alafs*35)	36%	2652X	NGSlyT	none
MEITL-63	3	47142980	C	G	missense_variant	3p21	SETD2	NM_014159.6	c.4983G>C (p.Glu1661Asp)	38%	2269X	NGSlyT	none
MEITL-63	X	39934182	TC	T	frameshift_variant	Xp11	BCOR	NM_001123383.1	c.416del (p.Gly139Glufs*22)	63%	3629X	NGSlyT	none
MEITL-64	11	108196144	G	A	missense_variant	11q22	ATM	NM_000051.3	c.6680G>A (p.Arg2227His)	92%	1461X	NGSlyT	none
MEITL-64	3	47165583	TG	T	frameshift_variant	3p21	SETD2	NM_014159.6	c.542del (p.Thr181Lysfs*3)	37%	4236X	NGSlyT	none
MEITL-65	17	40359729	T	G	missense_variant	17q21	STAT5B	NM_012448.3	c.1924A>C (p.Asn642His)	53%	2012X	NGSlyT	none
MEITL-65	3	47079266	G	A	stop_gained&splice_region_variant	3p21	SETD2	NM_014159.6	c.7240C>T (p.Gln2414*)	38%	1719X	NGSlyT	none
MEITL-65	3	47165754	TA	T	frameshift_variant	3p21	SETD2	NM_014159.6	c.371del (p.Leu124Tyrfs*28)	43%	2494X	NGSlyT	none
MEITL-65	X	39922122	G	GT	frameshift_variant&stop_gained	Xp11	BCOR	NM_001123383.1	c.3947dup (p.Tyr1316*)	5%	2917X	NGSlyT	none
MEITL-66	17	40354460	A	T	missense_variant	17q21	STAT5B	NM_012448.3	c.2135T>A (p.Val712Glu)	54%	1111X	NGSlyT	none
MEITL-66	17	7578406	C	T	missense_variant	17p13	TP53	NM_000546.5	c.524G>A (p.Arg175His)	40%	1296X	NGSlyT	none
MEITL-66	3	47142993	G	A	missense_variant	3p21	SETD2	NM_014159.6	c.4970C>T (p.Pro1657Leu)	25%	1739X	NGSlyT	none
MEITL-67	12	49415848	C	T	missense_variant	12q13	KMT2D	NM_003482.3	c.16499G>A (p.Arg5500Gln)	25%	1310X	NGSlyT	none
MEITL-67	17	7577058	C	A	stop_gained	17p13	TP53	NM_000546.5	c.880G>T (p.Glu294*)	89%	1000X	NGSlyT	none
MEITL-67	3	47165338	A	C	stop_gained	3p21	SETD2	NM_014159.6	c.788T>G (p.Leu263*)	35%	374X	NGSlyT	none
MEITL-67	X	41200862	A	AG	frameshift_variant&splice_region_variant	Xp11	DDX3X	NM_001356.4	c.281dup (p.Arg95Lysfs*3)	91%	487X	NGSlyT	none
MEITL-7	17	40359729	T	G	nonsynonymous SNV	17q21.2	STAT5B	NM_012448.3	c.1924A>C (p.Asn642His)	49.34%	1279X	NGSlyT; Nat Comm	none
MEITL-7	17	40370341	T	C	missense_variant	17q21	STAT5B	NM_012448.3	c.997A>G (p.Ile333Val)	38%	1423X	NGSlyT; Nat Comm	none
MEITL-7	3	47088072	G	A	stop_gained	3p21	SETD2	NM_014159.6	c.7003C>T (p.Gln2335*)	44%	1779X	NGSlyT; Nat Comm	none
MEITL-7	3	47165267	CA	C	frameshift_variant	3p21	SETD2	NM_014159.6	c.858del (p.Ile286Metfs*15)	40%	992X	NGSlyT; Nat Comm	none
MEITL-70	17	40354460	A	T	missense_variant	17q21	STAT5B	NM_012448.3	c.2135T>A (p.Val712Glu)	55%	969X	NGSlyT	none
MEITL-70	3	47088036	G	A	stop_gained	3p21	SETD2	NM_014159.6	c.7039C>T (p.Gln2347*)	26%	2695X	NGSlyT	none
MEITL-70	X	39923699	C	A	missense_variant	Xp11	BCOR	NM_001123383.1	c.3392G>T (p.Arg1131Leu)	53%	2414X	NGSlyT	none
MEITL-71	17	7577131	G	C	missense_variant	17p13	TP53	NM_000546.5	c.807C>G (p.Ser269Arg)	55%	784X	NGSlyT	none
MEITL-71	3	47165204	TAG	T	frameshift_variant	3p21	SETD2	NM_014159.6	c.920_921del (p.Ser307*)	33%	1244X	NGSlyT	none
MEITL-73	11	108141988	T	C	missense_variant	11q22	ATM	NM_000051.3	c.2932T>C (p.Ser978Pro)	14%	1812X	NGSlyT	none
MEITL-73	11	108235824	C	A	missense_variant	11q22	ATM	NM_000051.3	c.8866C>A (p.Pro2956Thr)	35%	2602X	NGSlyT	none
MEITL-73	17	40359729	T	G	missense_variant	17q21	STAT5B	NM_012448.3	c.1924A>C (p.Asn642His)	11%	2901X	NGSlyT	none
MEITL-73	3	47164413	AT	A	frameshift_variant	3p21	SETD2	NM_014159.6	c.1712del (p.Asn571Ilefs*8)	37%	3369X	NGSlyT	none
MEITL-73	3				missense_variant;frameshift_variant	3p21	SETD2	NM_014159.6	c.[354G>A; 360_366del] (p.[Met118Ile; Gly12	34%; 30%	2832X; 2589X	NGSlyT	none
MEITL-74	1	65312365	A	G	missense_variant	1p31	JAK1	NM_002227.3	c.1954T>C (p.Tyr652His)	11%	2421X	NGSlyT	none
MEITL-74	17	40359729	T	G	missense_variant	17q21	STAT5B	NM_012448.3	c.1924A>C (p.Asn642His)	24%	2441X	NGSlyT	none
MEITL-74	3	47161887	ACTCT	A	frameshift_variant	3p21	SETD2	NM_014159.6	c.4235_4238del (p.Glu1412Valfs*19)	12%	3963X	NGSlyT	none
MEITL-74	3	47165734	GA	G	frameshift_variant	3p21	SETD2	NM_014159.6	c.391del (p.Ser131Profs*21)	12%	3621X	NGSlyT	none
MEITL-74	7	2978338	C	T	missense_variant	7p22	CARD11	NM_032415.5	c.992G>A (p.Arg331His)	46%	1765X	NGSlyT	none
MEITL-74	X	39931909	G	A	missense_variant	Xp11	BCOR	NM_001123383.1	c.2690C>T (p.Ser897Leu)	47%	2641X	NGSlyT	none
MEITL-74	X	39932689	G	C	missense_variant	Xp11	BCOR	NM_001123383.1	c.1910C>G (p.Ser637Cys)	47%	2642X	NGSlyT	none
MEITL-9	11	108124663	A	G	missense_variant	11q22	ATM	NM_000051.3	c.2021A>G (p.His674Arg)	46%	399X	NGSlyT; Nat Comm	none
MEITL-9	11	108160506	T	G	missense_variant	11q22	ATM	NM_000051.3	c.4414T>G (p.Leu1472Val)	46%	312X	NGSlyT; Nat Comm	none
MEITL-9	17	40354460	A	T	missense_variant	17q21	STAT5B	NM_012448.3	c.2135T>A (p.Val712Glu)	37%	190X	NGSlyT; Nat Comm	none
MEITL-9	17	40359729	T	G	missense_variant	17q21	STAT5B	NM_012448.3	c.1924A>C (p.Asn642His)	32%	351X	NGSlyT; Nat Comm	none
MEITL-9	3	47147507	T	C	missense_variant	3p21	SETD2	NM_014159.6	c.4819A>G (p.Met1607Val)	60%	230X	NGSlyT; Nat Comm	none
MEITL-202	3	47139440	C	T	splicing_variant		SETD2	NM_014159.6	c.5142+5G>A	9.4%	395X	V1	none

‡ Panel legend

Nat Comm : TDS with 9 genes (*CREBB, JAK1, JAK2, JAK3, SETD2, STAT5B, STAT1, STAT3, STAT5A*) used in the Nature communication publication of Roberti et al. 2016 (1).
V1 : TDS with 9 genes (*CD28, DNMT3A, IDH2, PLCG1, RHOA, SETD2, STAT3, STAT5B, TET2,*) as previously described[4.]

NGSlyT: TDS with 27 genes (*ARID1A, ATM, BCOR, CARD11, CCR4, CD28, CTNNB1, DDX3X, DNMT3A, FYN, IDH2, IRF4, JAK1, JAK3, KMT2D, PIK3CD, PLCG1, PRKCB, RHOA, SETD2, SOCS1, STAT3, STAT5B, TET2, TNFRSF1B, TP53, VAV1*) as described in "Material and Methods" of the main manuscript.

Exome.IDT : Whole exome sequencing perfromed with IDT probes as described in "Material and Methods" of the main manuscript

Exome.Ag: Whole exome sequencing perfromed with Agilent probes and used in the Nature communication publication of Roberti et al. 2016[1.]

Supplementary Table S6. Univariate analysis of overall survival in MEITL (n=63).

Characteristics	n (%)	median OS	*P*	HR	CI
Age (years)					
<70	38 (60.3%)	9.7	**0.039**	1.75	1.03-2.98
≥70	25 (39.7%)	3.3.			
Gender					
Male	31 (49.2%)	8.4	0.788	1.07	0.64-1.82
Female	32 (50.8%)	5.8			
Bowel perforation					
No	17 (27.9%)	10.8	0.484	1.24	0.68-2.28
Yes	44 (72.1%)	5.8			
Surgical procedure					
Anastomosis	24 (61.5%)	10.3	**0.015**	2.43	1.19-4.97
Enterostomy	15 (38.5%)	5.2			
PS					
0-2	42 (75%)	10.8	**<0.005**	4.46	2.15-9.28
3-4	14 (25%)	3.9			
Lugano stage					
1	21 (35%)	17.3	**0.025**	1.96	1.09-3.54
≥2	39 (65%)	5.7			
Response to first-line chemotherapy					
CR	15 (35.7%)	21.1	**<0.005**	5.85	2.66-12.88
non-CR	27 (64.3%)	7.9			
Cytology					
Monomorphic	47 (74.6%)	10.3	**0.013**	2.12	1.17-3.85
Non-monomorphic	16 (25.4%)	4.3			
Necrosis					
No	54 (85.7%)	7.9	0.61	1.2	0.59-2.46
Yes	9 (14.3%)	5.2			
Starry-sky/apoptosis					
No	56 (88.9%)	8.3	0.27	1.6	0.68-3.76
Yes	7 (11.1%)	1.1			
Angiotropism/angioinvasion					
No	41 (71.9%)	9.7	**0.034**	1.9	1.05-3.57
Yes	16 (28.1%)	5.2			
Atypical histology					
No	36 (57.1%)	10.8	**0.011**	2.00	1.17-3.41
Yes	27 (42.9%)	5.2			
Ki-67					
≤50%	18 (29.5%)	7.9	0.809	1.08	0.59-1.96
>50%	43 (70.5%)	5.8			
CD56					
Negative	7 (11.1%)	3.4	0.208	0.60	0.27-1.33
Positive	56 (88.9%)	7.9			
TCR β					
Negative	40 (70.2%)	7.9	0.290	1.38	0.76-2.52

Positive	17 (29.8%)	5.6			
TCRγδ					
Negative	28 (50%)	7.9	0.575	1.17	0.67-2.05
Positive	28 (50%)	5.2			
TCR expression status					
Silent	15 (27.8%)	7.9	0.594	1.20	0.62-2.31
Expressed	39 (72.2%)	5.6			
B-cell marker expression					
Negative	48 (77.4%)	7.8	**0.046**	0.49	0.24-0.99
Positive	14 (22.6%)	12.4			
MYC expression (IHC)					
No (<25%)	34 (68%)	9.7	**0.005**	2.56	1.33-4.95
Yes (25-100%)	16 (32%)	3.4			
***MYC* gene (FISH)**					
Normal FISH pattern	46 (82.1%)	7.9	0.150	1.72	0.82-3.59
Copy gain or rearrangement	10 (17.9%)	3.4			
H3K36 trimethylation					
Normal	5 (8.5%)	10.3	0.558	0.76	0.30-1.92
Defective	54 (91.5%)	5.8			
p53 expression (IHC)					
Wild type pattern	35 (67.3%)	9.5	0.244	1.44	0.78-2.66
Mutated pattern	17 (32.7%)	5.6			
***TP53* mutation**					
No	38 (66.7%)	9.7	**0.016**	2.11	1.15-3.87
Yes	19 (33.3%)	5.6			
***STAT5B* mutation**					
No	22 (38.6%)	10.3	0.101	1.6	0.91-2.90
Yes	35 (61.4%)	4.3			
***TP53/STAT5B* mutation(s)**					
Both wild-type	13 (22.8%)	13.7			
TP53 or *STAT5B* mutation	35 (61.4%)	5.6	**0.058**	2.00	0.98-4.12
TP53 and *STAT5B* mutations	9 (15.8%)	1.8	**0.007**	3.54	1.41-8.87
***JAK3* mutation**					
No	30 (53.6%)	5.6	0.303	0.74	0.42-1.31
Yes	26 (46.4%)	5.8			
***JAK1* mutation**					
No	50 (89.3%)	5.7	0.293	1.60	0.67-3.82
Yes	6 (10.7%)	2.9			
***ATM* mutation**					
No	49 (89.1%)	5.7	0.660	0.81	0.32-2.06
Yes	6 (10.9%)	1.1			
***BCOR* mutation**					
No	47 (87%)	5.6	0.534	1.30	0.57-2.93
Yes	7 (13%)	9.7			
***SETD2* mutation**					
Yes	51 (89.5%)	1.1	0.150	1.9	0.79-4.47
No	6 (10.5%)	7.9			

Abbreviations: CR, complete response; PS, Performance Status; FISH, fluorescent in situ hybridization; IHC, immunohistochemistry.

Estimates of overall survival were constructed using the Kaplan-Meier method. Cox proportional hazards regression model was used to investigate associated prognostic factors in univariate analysis. Results were expressed as hazard-ratio (HR) and 95% confidence interval. Statistical analysis was performed using Stata software. The tests were two-sided, with a type I error set at 5%. A Sidak's type I error correction was applied to consider multiple comparisons.

Supplementary Table S7. Detailed multivariable analysis.

	Multivariable analyses						***Sensitivity analysis***		
N=44	***Final model analysis***			***Bootstrap analysis***					
	HR	**95% CI**	***P value***	**HR**	**95% CI**	***P value***	**HR**	**95% CI**	***P value***
B-cell marker expression	0.15	0.05 – 0.46	0.001	0.15	0.03 – 0.85	0.032	0.15	0.04 – 0.55	0.004
***TP53* mutation**	4.86	1.75 – 13.5	0.002	4.86	1.25 – 18.9	0.022	4.85	1.73 – 13.6	0.003
***STAT5B* mutation**	3.42	1.44 – 8.13	0.005	3.42	1.03 – 11.4	0.045	3.40	1.40 – 8.26	0.007
MYC expression (IHC)	3.06	1.33 – 7.04	0.009	3.06	1.02 – 9.2	0.046	3.07	1.30 – 7.27	0.011
Performance Status ≥2	6.46	2.44 – 17.1	<0.001	6.46	2.06 – 20.2	0.001	6.64	2.41 – 18.2	<0.001
Age ≥70	NA	NA	NA	NA	NA	NA	0.98	0.43 – 2.20	0.953
Lugano stage ≥2	NA	NA	NA	NA	NA	NA	1.08	0.44 – 2.65	0.865

NA: not assessed.

Supplementary Table S8. Characteristics of long survivor patients

MEITL No	OS (months) ; status	Age	Clinical Presentation	Stage	Localizations	PS	Surgery	Treatment	Response	Relapse	Atypical histology	IHC	*MYC gene* alteration	*TP53 mutation*	*STAT5B mutation*	*SETD2 mutation*	Other mutations
41	29 ; Alive, CR	69	Occlusion	1	Small bowel, large bowel	1	+	CHOP	CR	-	-	CD2- CD4- CD8+ CD56+ TCR- CD20- CD79a- MYC- p53-	-	-	-	+	*JAK3 GNAI2 TET2*
69	32 ; Dead (disease)	66	Perforation	1	Small bowel	1	+	CHOP	CR	+	-	CD2- CD4- CD8+ CD56+ CD20- MYC-	ND	ND	ND	ND	ND
42	45, Alive, CR	63	Perforation	4	Small bowel, abdominal wall, pelvic tumor	1	+	CHOEP	CR	-	+	CD2+ CD4- CD8+ CD56+ TCRγδ CD20+ CD79a+ MYC- p53-	-	-	+	+	-
23	46 ; Dead (disease)	72	Perforation	4	Small bowel, abdominal wall, bladder	2	+	CHOP	PR	+	+	CD2- CD4- CD8+ CD56+ TCR- CD20- CD79a- MYC- p53+	-	-	+	+	*JAK3*
35	47 ; Alive, CR	68	Perforation	1	Small bowel, large bowel	1	+	CHOP	CR	-	-	CD2+ CD4+ CD8+ CD56+ TCRβ CD20+ CD79a- MYC- p53-	-	-	-	+	*JAK3*
34	55 ; Alive, CR	90	Perforation	1	Small bowel	1	+	-	CR	-	-	CD2+ CD4- CD8+ CD56+ TCRγδ CD20+ CD79a- MYC- p53-	-	-	+	+	*ATM PIK3CD*
27	69 ; Alive, CR	66	Perforation	4	Small bowel, lung, tongue	0	+	CHOP + IVE-MTX	CR	+	-	CD2+ CD4- CD8+ CD56+ CD20+ CD79a- MYC- p53-	ND	-	-	+	*JAK3 PLCG1*
30	71 ; Dead (disease)	46	ND	ND	ND	ND	+	ND	ND	+	-	CD2- CD4- CD8- CD56+ TCR- CD20- MYC- p53-	-	-	+	+	*JAK3*

Abbreviations: CHOP, Cyclophosphamide, Doxorubicin, Vincristine, Prednisone; CHOEP, Cyclophosphamide, Doxorubicin, Vincristine, Etoposide, Prednisone; CR, complete response; IVE-MTX, Ifosfamide, Epirubicin, Etoposide, Methotrexate; ND, no data; OS: overall survival; PR, partial response

Supplementary Figures

Supplementary Figure S1. Digital database designed to record the morphological features, immunohistochemical and FISH results of MEITL cases.

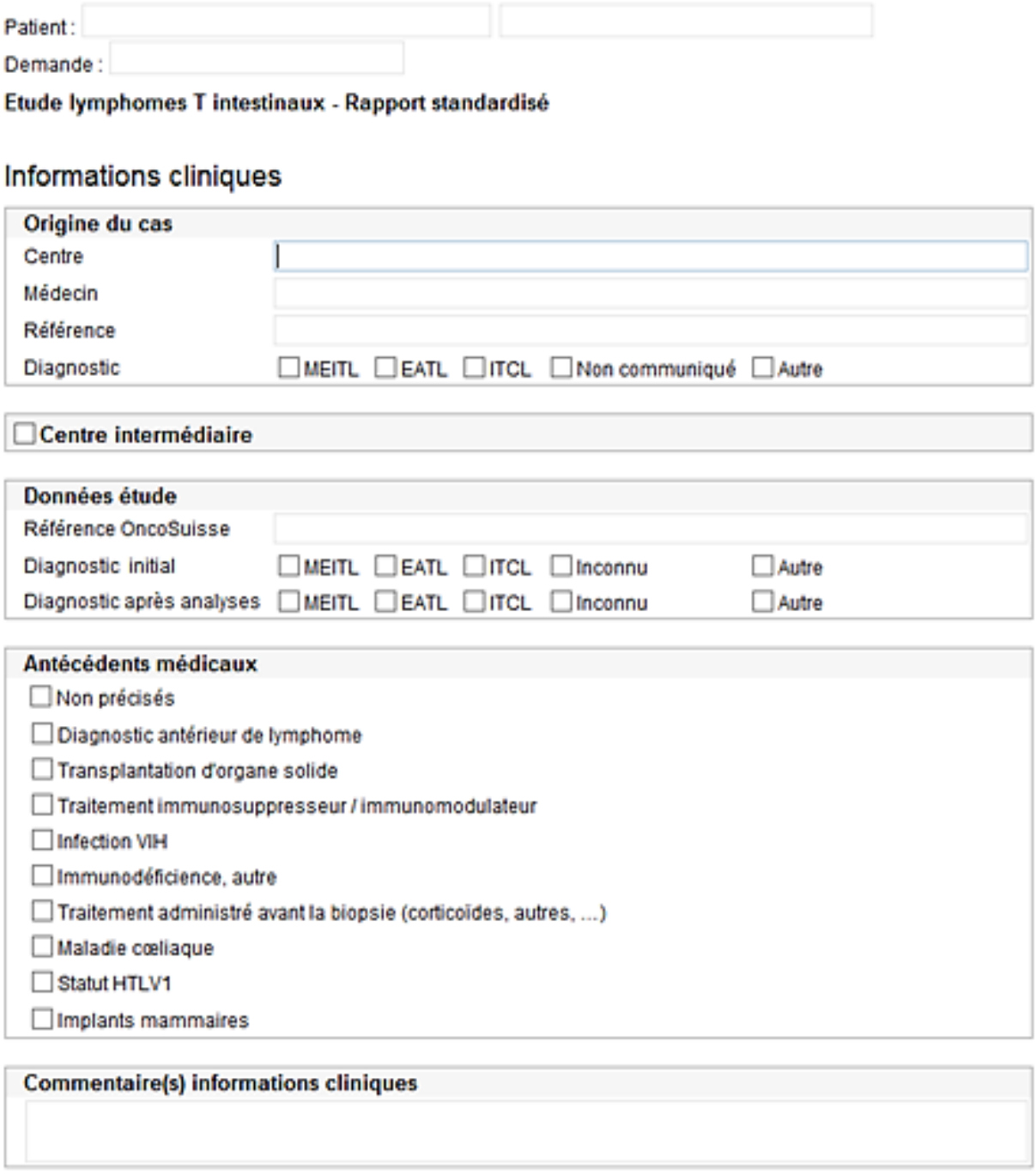
Patient :

Demande :

Etude lymphomes T intestinaux - Rapport standardisé

Informations cliniques

Origine du cas

Centre

Médecin

Référence

Diagnostic ☐ MEITL ☐ EATL ☐ ITCL ☐ Non communiqué ☐ Autre

☐ **Centre intermédiaire**

Données étude

Référence OncoSuisse

Diagnostic initial ☐ MEITL ☐ EATL ☐ ITCL ☐ Inconnu ☐ Autre

Diagnostic après analyses ☐ MEITL ☐ EATL ☐ ITCL ☐ Inconnu ☐ Autre

Antécédents médicaux

☐ Non précisés

☐ Diagnostic antérieur de lymphome

☐ Transplantation d'organe solide

☐ Traitement immunosuppresseur / immunomodulateur

☐ Infection VIH

☐ Immunodéficience, autre

☐ Traitement administré avant la biopsie (corticoïdes, autres, ...)

☐ Maladie cœliaque

☐ Statut HTLV1

☐ Implants mammaires

Commentaire(s) informations cliniques

Matériel

Description

Nombre de lames

Nombre de blocs

Ajouter un bloc ré-encodé

Examen macroscopique

Type de prélèvement

- [ ] Ganglion(s) lymphatique(s)
- [ ] Rate
- [ ] Médiastin
- [ ] Moelle osseuse
- [ ] Peau
- [ ] Organes digestifs (préciser)
- [ ] Epiploon
- [ ] Autre

Latéralité de l'échantillon

- ○ Non applicable
- ○ Non précisée
- ○ Gauche
- ○ Droite

Type de procédure

- ○ Biopsie chirurgicale
- ○ Biopsie à l'aiguille
- ○ Résection chirurgicale
- ○ Résection endoscopique
- ○ Ponction cytologique
- ○ Autre
- ○ Non précisé

Taille de la lésion

Taille (cm) Préciser ☐ Non communiquée

Commentaire(s) examen macroscopique

Examen microscopique

Tissu lésionnel

Infiltration

- ☐ Muqueuse
- ☐ Sous-muqueuse
- ☐ Musculeuse
- ☐ Tissu adipeux et/ou péritoine
- ☐ Autre

Perforation

- ○ Présente
- ○ Absente
- ○ Non évaluable
- ○ Autre

Ulcération

- ○ Présente
- ○ Absente
- ○ Non évaluable
- ○ Autre

Infiltration ganglionnaire

- ○ Présente
- ○ Absente
- ○ Non évaluable
- ○ Autre

Nécrose

Nécrose (%) Préciser

" Fat rimming "

- ○ Présent
- ○ Absent
- ○ Non évaluable
- ○ Autre

Cytologie & Patterns

Morphologie cellulaire	○ Monomorphe	○ Pléomorphe	○ Autre
Anaplasique	○ Absent	○ Minorité de cellules tumorales	○ Majorité de cellules tumorales
Blastoïde	○ Absent	○ Minorité de cellules tumorales	○ Majorité de cellules tumorales
"Starry sky"	○ Absent	○ Focal	○ Extensif

☐ Autre

Epithéliotropisme

- ○ Présent
- ○ Absent
- ○ Non évaluable
- ○ Autre

Angiotropisme

- ○ Présent
- ○ Absent
- ○ Non évaluable
- ○ Autre

Inflammation

Inflammation (%) Préciser

Commentaire Préciser

Taille cellulaire

- ☐ Petite
- ☐ Moyenne
- ☐ Grande
- ☐ Autre

Commentaire(s)

Paroi à distance

Entéropathie

- ○ Présente
- ○ Absente
- ○ Non évaluable

Lymphome intra-épithélial

- ○ Présent
- ○ Absent
- ○ Non évaluable

Marges de résection

- ○ Non applicable
- ○ RX: Ne peuvent être évaluées
- ○ R0: Marges exemptes de tumeur
- ○ R1: Marges positives microscopiques
- ○ R2: Marges positives macroscopiques

Autre(s) observation(s) microscopique(s)

- ☐ Hyperplasie lymphoïde
- ☐ Inflammation chronique
- ☐ Autre

Commentaire(s)

Immunophénotype / Biomarqueurs

Immunohistochimie

- ☐ Tumeur
- ☐ Lymphocytes intra-épithéliaux
- ☐ Lymphome intra-épithélial

Analyses génétiques / moléculaires

Analyses FISH

- ○ Non effectuée(s)
- ○ Effectuée(s)

Recherche de clonalité lymphoïde

- ○ Non effectuée
- ○ Effectuée

☐ Elément(s) d'intérêt didactique

Utilisation du cas

- ☐ TMA
- ☐ Séquençage DNA
- ☐ Méthylome
- ☐ RNAseq
- ☐ IEL à distance: cas éligible pour analyse(s)
- ☐ Autre

Commentaire(s)

Commentaire(s) supplémentaire(s)

Supplementary Figure S2. MEITL in non-intestinal organs. MEITL with anal involvement (MEITL 44, A-D), MEITL with lymph node involvement (MEITL 53, E-F) and massive involvement of the bone marrow (MEITL 16, G-H).

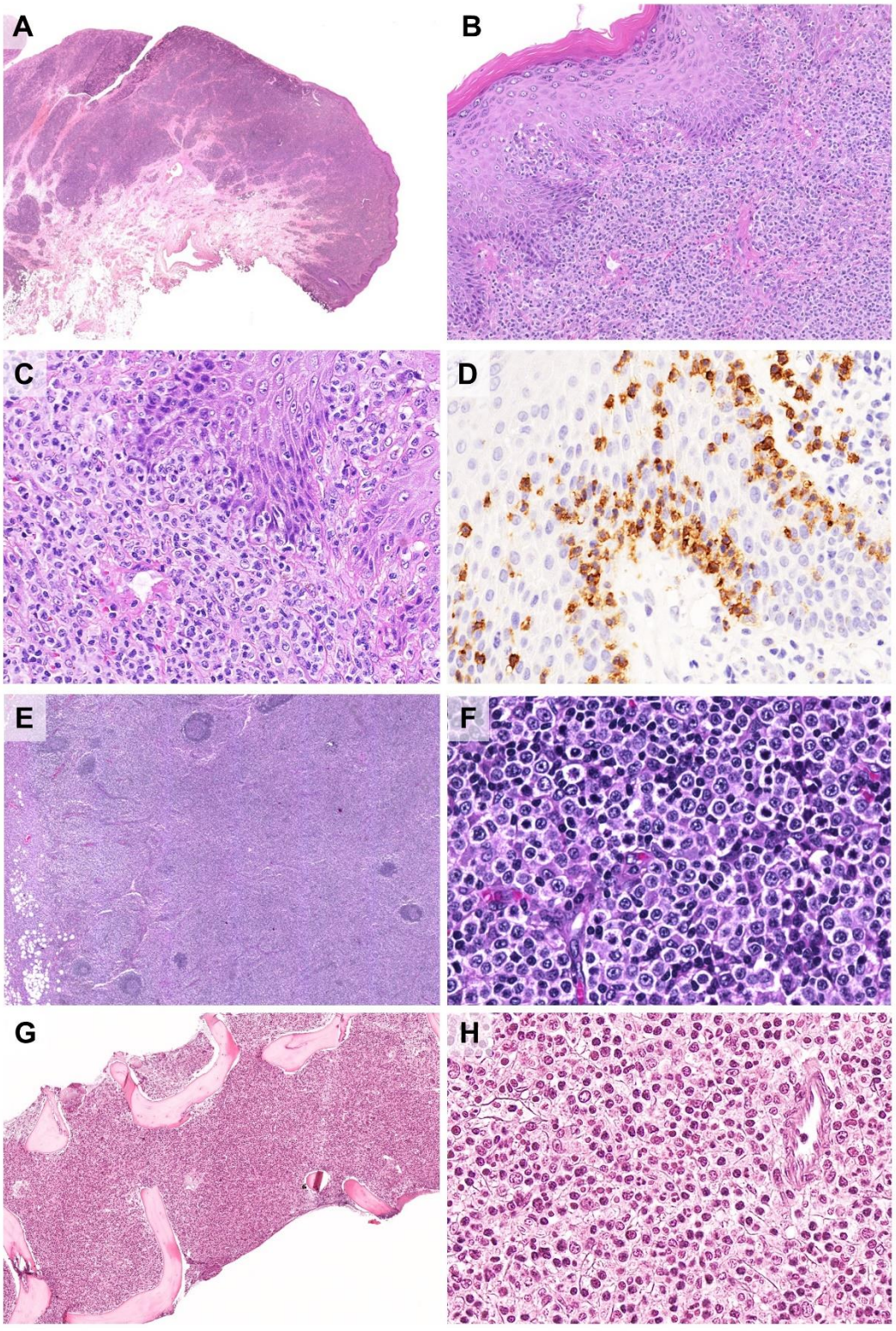

(A) This case shows a diffuse and dense infiltrate of tumor cells involving the entire thickness of the skin, and focally the subcutaneous fat, with surface ulceration. **(B** and **C)** Tumor cells show important epitheliotropism in the squamous epithelium of anal mucosa. **(D)** Epitheliotropic tumor cells are strongly positive for CD103. **(E)** Lymph node involved by MEITL shows a massive infiltration of paracortex with some residual B-cell follicles. **(F)** Tumor cells show a non-monomorphic cytology with intermediate/large sized tumor cells, many with evident nucleoli and ample cytoplasm. **(G)** This case shows a packed bone marrow with an extensive tumor infiltration. **(H)** Tumor cells display a monomorphic cytology. Original magnifications: x12.5 (A), x25 (E), x50 (G), x100 (B), x400 (C, D, F, H).

Supplementary Figure S3. MEITL with peculiar immunophenotypes (with B-cell antigen expression (case 42, A-C), with MYC expression (case 2, D-F) and double positive for TCR isoforms (case 56, G-I).

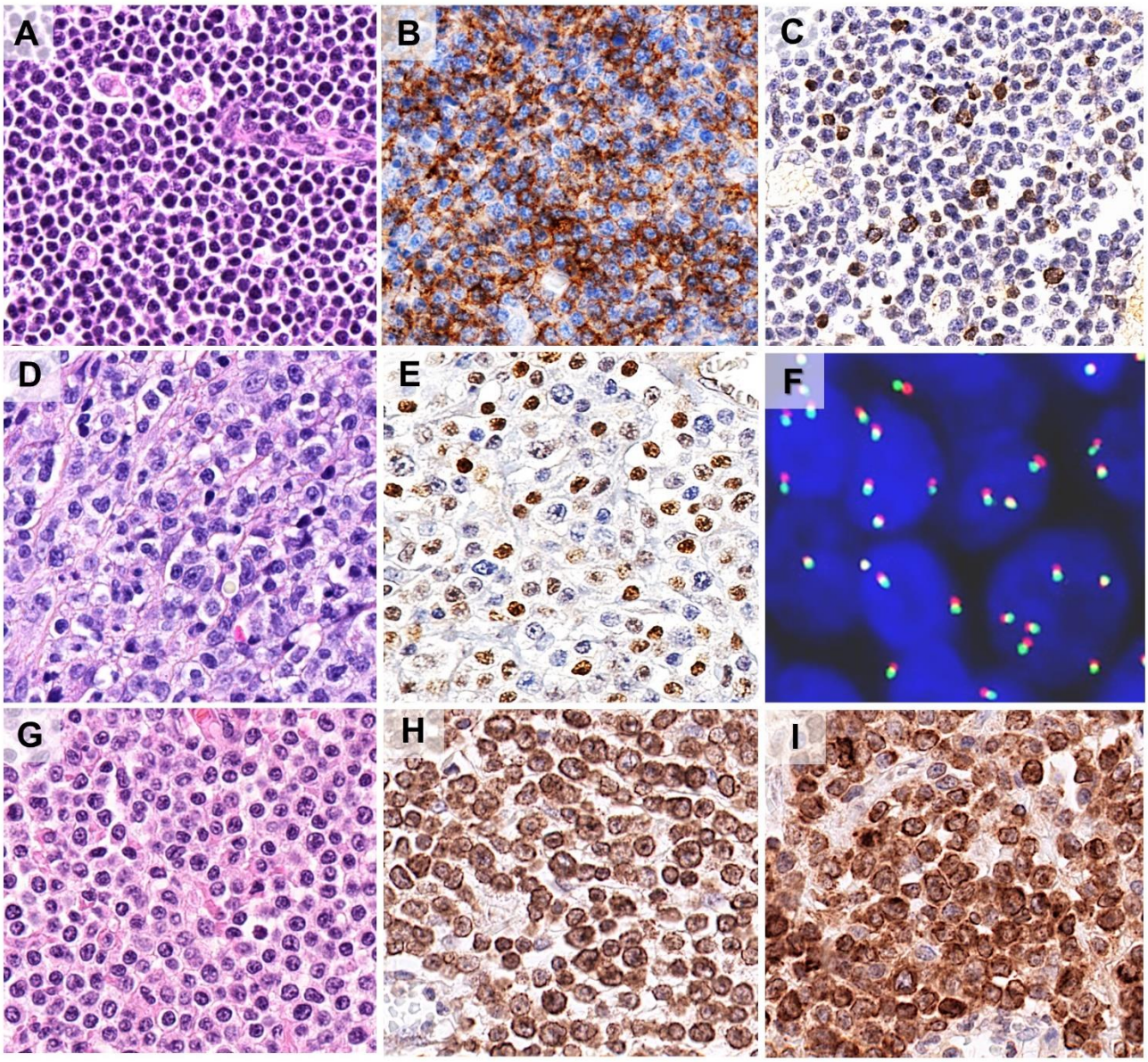

(A) This tumor shows an atypical “starry-sky” pattern. **(B)** Tumor cells are diffusely positivity for CD20. **(C)** CD79a is expressed in occasional atypical tumor cells. **(D)** Intermediate/large-sized tumor cells show nuclear pleomorphism and conspicuous nucleoli. **(E)** MYC was positive in most tumor cells. **(F)** *MYC* FISH shows many tumor cells with gene copy gains (3-6 signals/nucleus). **(G)** This tumor is composed of intermediate-sized tumor cells with clear cytoplasm and slight nuclear irregularity. **(H)** The

lymphoma cells were positive for TCRβ, and **(I)** TCRδ. Original magnifications: ×400 (A-E,G-I), x630 (F).

Supplementary Figure S4. Morphological, immunophenotypical and genetic characteristics of atypical MEITL case No. 66.

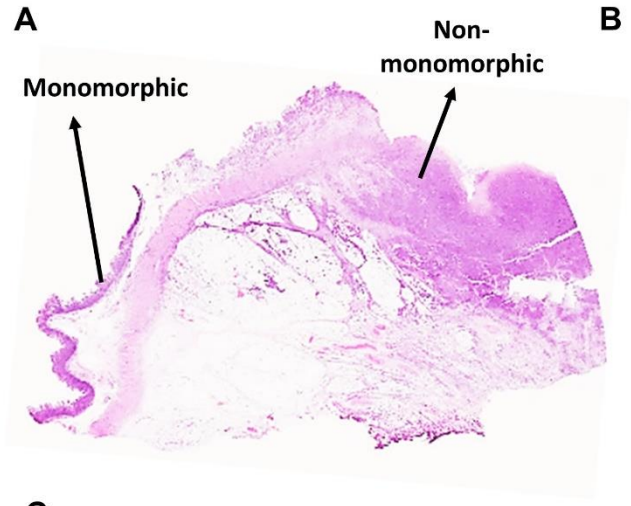

B

	Monomorphic	Non-monomorphic
IHC		
CD4	+	+
CD8	-	+
CD56	-	+
TIA1	-	+
Ki-67	15%	50%
CD30	<1%	~15%
Genetics		
STAT5B (p.Val712Glu) VAF	64	54
TP53 (p.Arg175His) VAF	45	40
SETD2 (p.Pro1657Leu) VAF	28	25
MYC FISH	Normal	Rearrangements (49%)

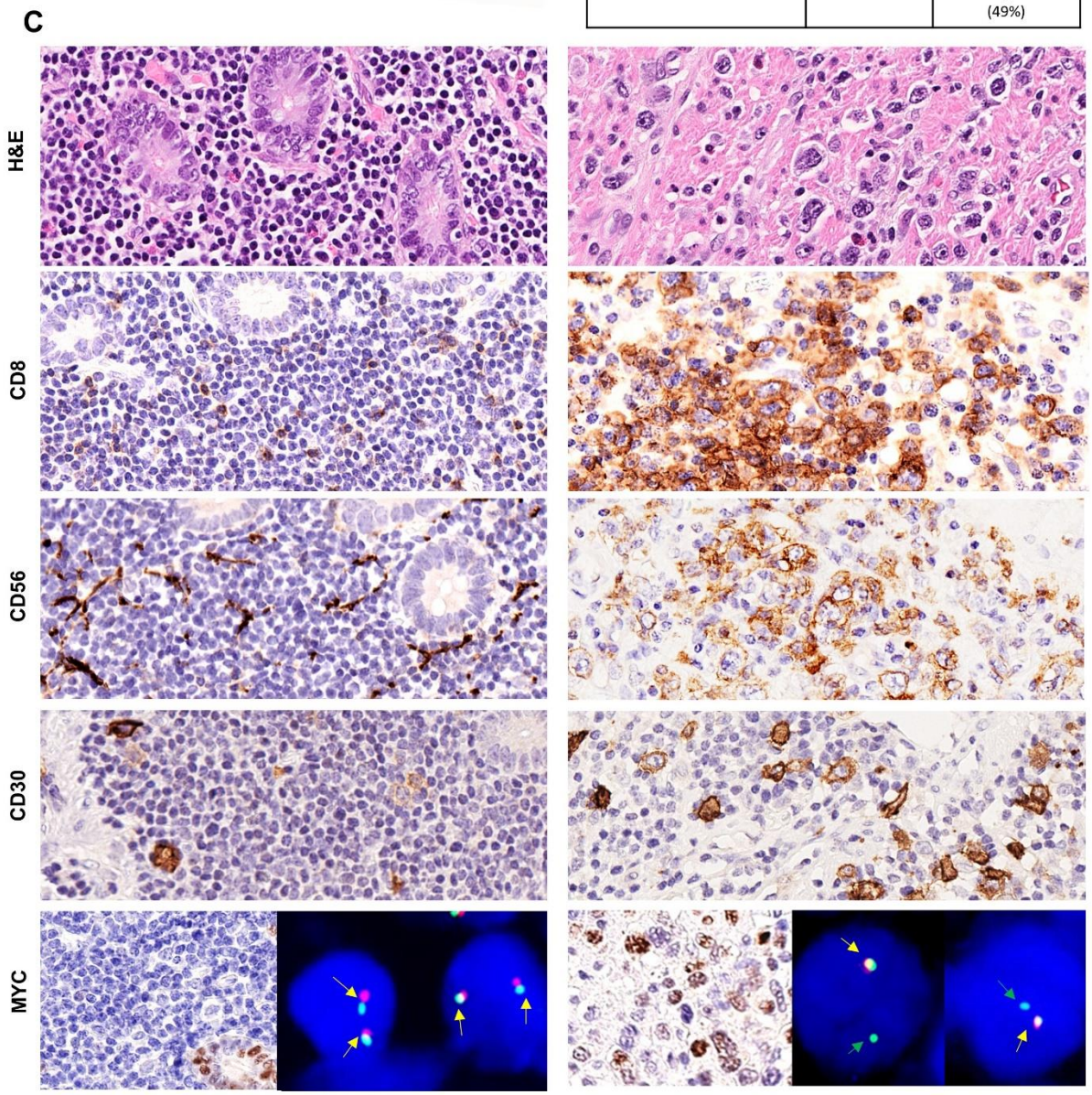

(A) This case shows two well-defined tumor areas: one corresponding to the intramucosal component of the peripheral zone, composed of small and round lymphocytes with a monomorphic cytology (left). The other area represents the central zone characterized by a non-monomorphic cytology with many large cells reminiscent of Hodgkin and Reed-Sternberg cells (right). **(B** and **C)** The two areas display distinctive immunophenotypic profiles: tumor cells with monomorphic cytology show an atypical immunophenotype: CD4+, CD8-, CD56-, TIA1-, are CD30- and show low proliferation (Ki-67~15%). In contrast, the non-monomorphic component is CD4+, CD8+, CD56+, TIA1+, CD30-/+ and display a higher proliferation (Ki-67 50%). Although cytologically and immunophenotypically different, which suggested initially the co-occurrence of two different types of T-cell lymphoma, an identical mutational profile (*SETD2, TP53* and *STAT5B* mutations at similar VAF) was observed, which confirmed the clonal relationship of both component and also diagnosis of MEITL in the two areas. Interestingly, *MYC* FISH study shows a pattern compatible with a gene rearrangement in the non-monomorphic component (49% of nuclei showed a loss of one red signal), which is associated with MYC overexpression (bottom right). On the contrary, *MYC* FISH study is normal in the monomorphic component, which is negative for MYC by immunohistochemistry (bottom left). Original magnifications: x400 (H&E, IHC in C), x630 (FISH in C).

Supplementary Figure S5. MEITL (#49) with preserved H3K36me3 trimethylation associated with the lack of *SETD2* gene alterations.

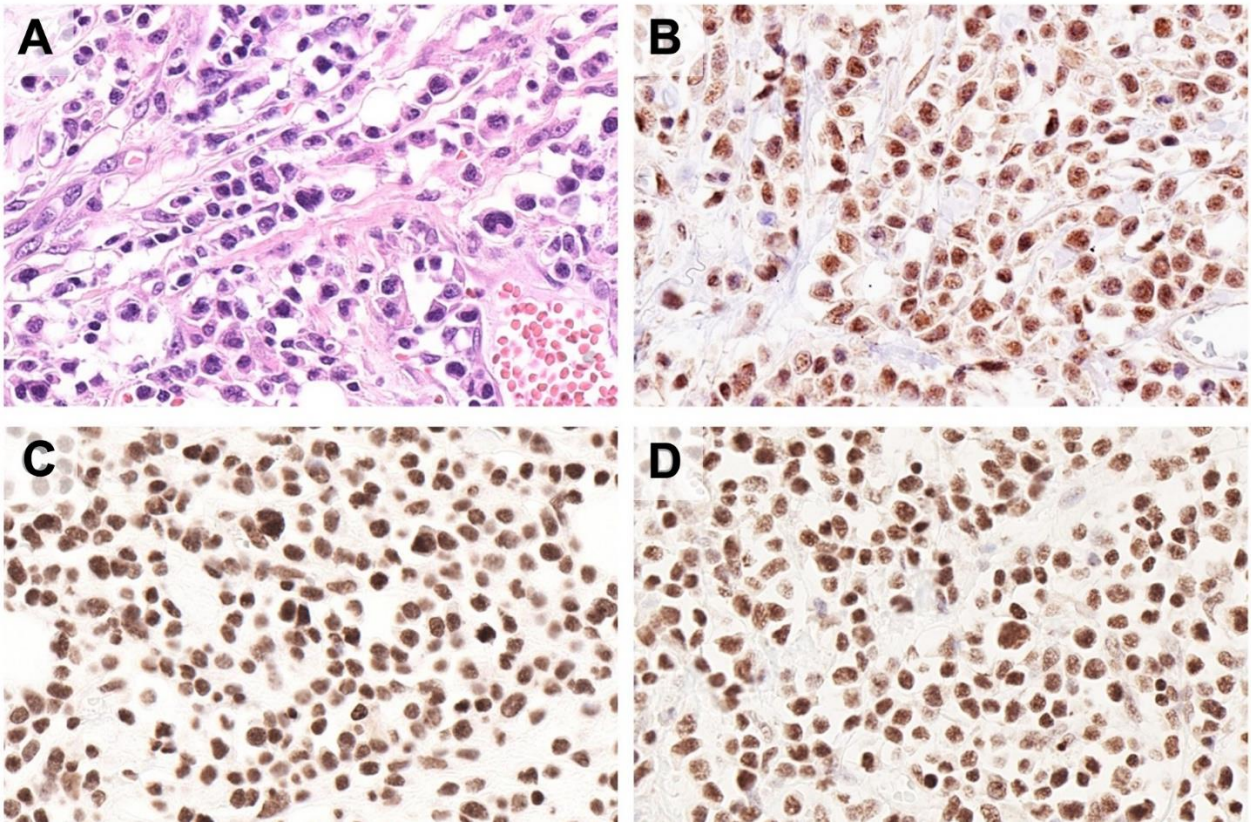

Exceptional case of MIETL with preserved H3K36me3 trimethylation. **(A)** The lymphoma cells show a non-monomorphic cytology, and **(B)** strong nuclear positivity for SETD2, and **(C)** H3K36me2, and **(D)** preserved expression of H3K36me3.

Supplementary Figure S6. Allele frequencies and loss of heterozygosity status observed for *JAK3*, *SETD2*, *STAT5B* and *TP53* mutations.

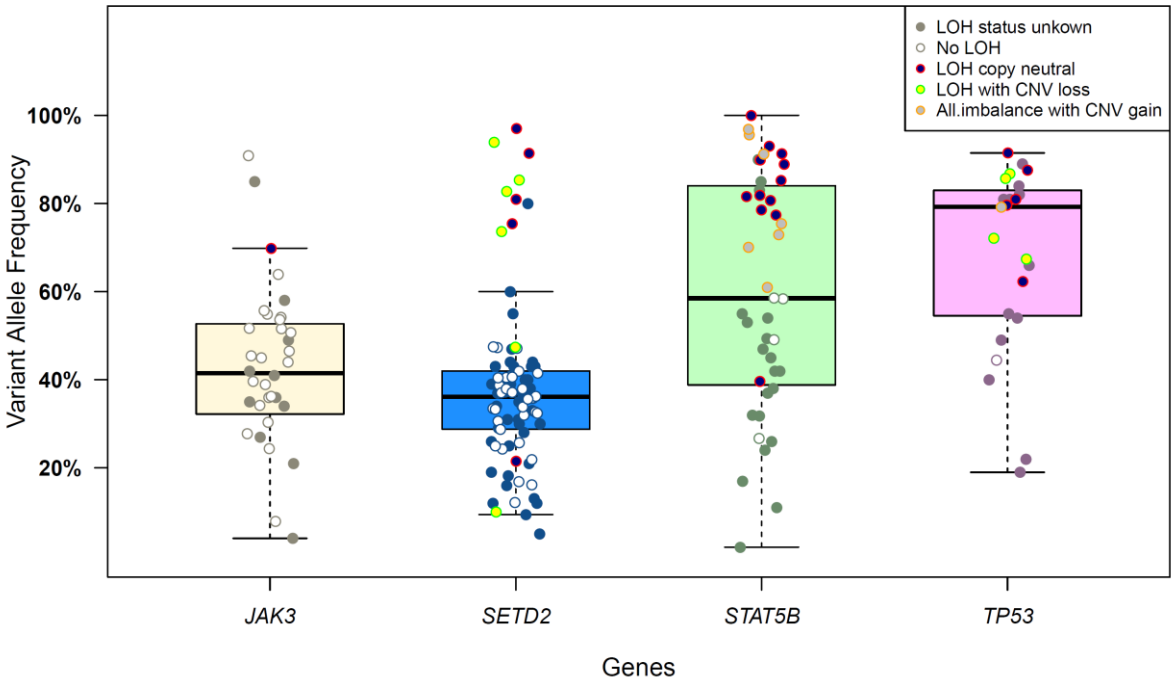

Box and whisker plot showing the distribution of allele frequencies observed for mutations in *JAK3*, *SETD2*, *STAT5B* and *TP53* genes. In addition, copy number variations as well as loss of heterozygosity (LOH) status were assessed from the 34 samples for which WES were performed. These co-occurring alterations were pointed in the plot with specific marks, as reported in the legend figure on the top right corner. Overall, of the 24 mutations observed in *STAT5B* by WES analysis, 23 (96%) had co-occurring LOH or allelic imbalance events (12 neutral, 7 with a CNV gain and 1 with CNV loss of the *STAT5B* locus) as previously observed (1). For *TP53*, out of the 11 mutations detected by WES, 10 (91%) were also associated with LOH (5 neutral, 4 with a CNV loss and 1 with CNV gain of the *TP53* locus). In comparison, *JAK3* (3/25 – 12%) and *SETD2* (12/45 – 27%) showed a significant lower number of LOH or allelic imbalance events associated with their mutations (for all comparison $p<0.001$, Fisher's exact test, while no statistical differences were observed between *STAT5B versus TP53* and *JAK3 versus SEDT2*). The

allele frequencies were also statistically significantly higher for mutations detected in *STAT5B* and *TP53* when compared with *SETD2* (both $p<0.001$, Wilcoxon rank sum test) and *JAK3* ($p<0.005$ and $p<0.001$, respectively). Again, no difference were observed between *STAT5B* and *TP53*, while a marginal higher allele frequencies was seen in *JAK3* versus *SEDT2* ($p=0.017$).

Supplementary Figure S7. Sankey plot of treatment and outcome of 63 MEITL patients

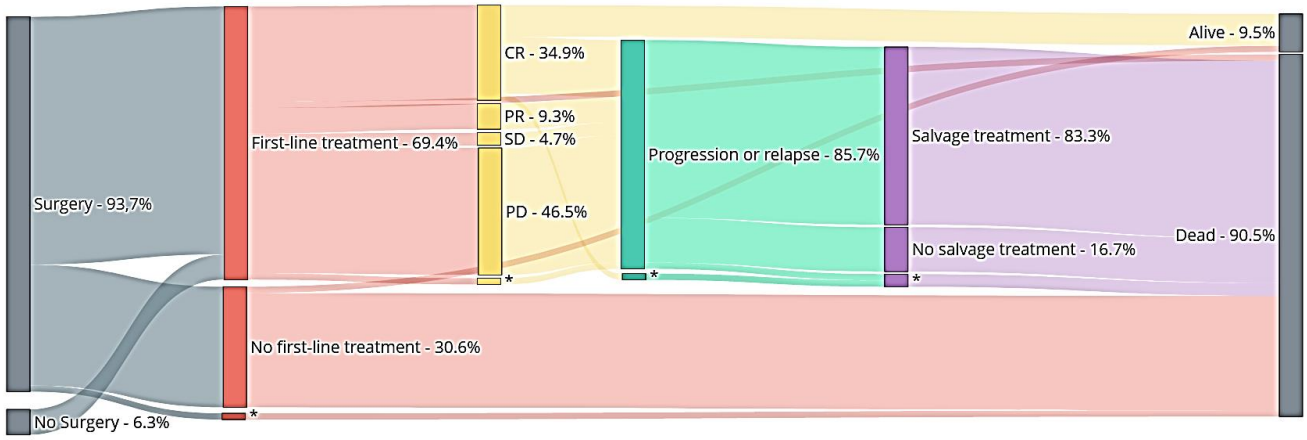

*Abbreviations: CR, complete remission; PR, partial response; SD, stable disease; PD, progressive disease, * unknown information.*

The height of flows is proportional to the number of patients. The length of flows is not proportional to time. Missing data/unknown information are not included in percentages. The median time between surgery and first-line treatment was 33 days with a range of 11 to 153 days. 57 patients died in a median time of 5.7 months (0-71 months), and 6 patients are alive and in complete remission at a median time of 45.8 months from diagnosis (5.6-69 months). The follow-up was 7.8 months for the whole cohort and 45.8 months in survivors. Abbreviations: CR, complete remission; PR, partial response; SD, stable disease; PD, progressive disease, * unknown information.

Supplementary Figure S8. Overall survival in MEITL according to treatment received and TCR expression.

A

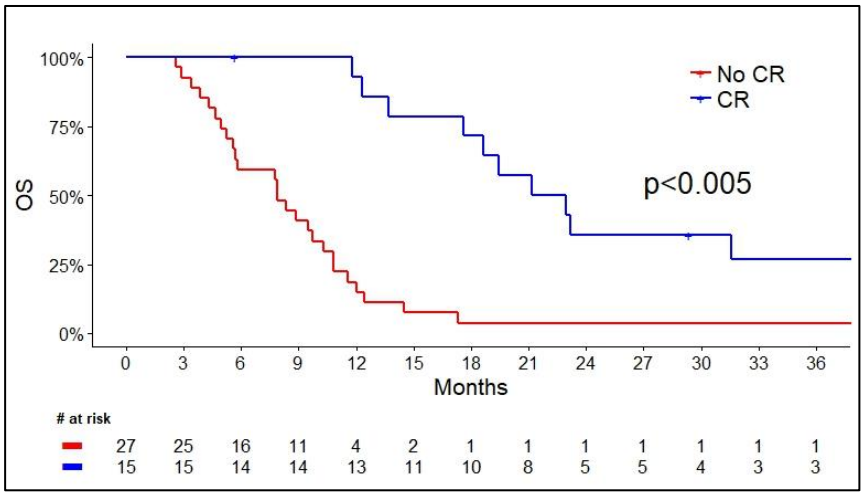

B

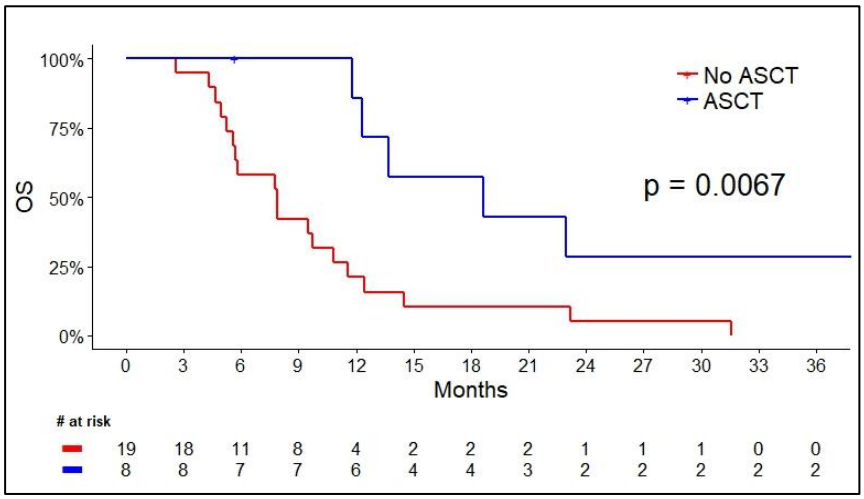

C

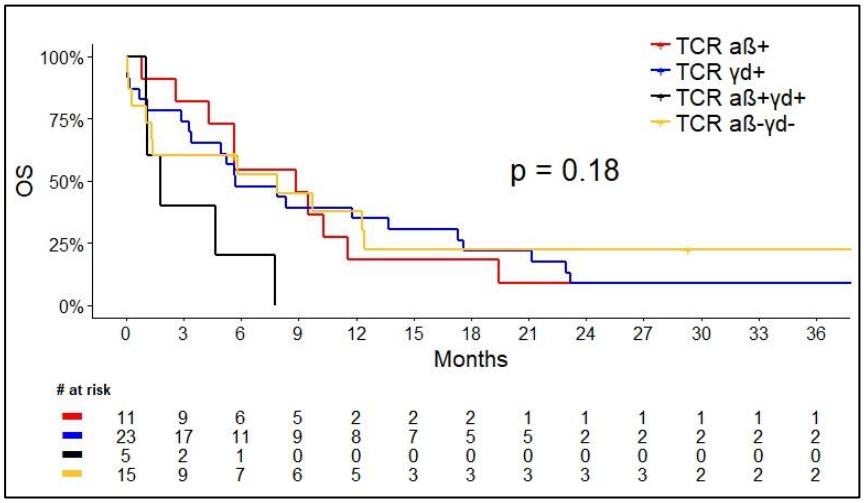

(A) Overall survival in months according to the response to first-line treatment, **(B)** according to ASCT in patients receiving a first-line treatment and younger than 67 years

old at diagnosis**,** and **(C)** according to the TCR expression. *Abbreviations: CR, complete response; OS, Overall Survival; ASCT, autologous stem cell transplantation*

References

1. Roberti A, Dobay MP, Bisig B, et al. Type II enteropathy-associated T-cell lymphoma features a unique genomic profile with highly recurrent SETD2 alterations. Nat commun. 2016;7:12602.

2. Trimech M, Letourneau A, Missiaglia E, et al. Angioimmunoblastic T-Cell Lymphoma and Chronic Lymphocytic Leukemia/Small Lymphocytic Lymphoma: A Novel Form of Composite Lymphoma Potentially Mimicking Richter Syndrome. Am J Surg Pathol. 2021;45(6):773-786.

3. Fajardo KF, Adams D, NISC Comparative Sequencing Program; Mason CE, Sincan M, Tifft C, et al. Detecting false-positive signals in exome sequencing. Hum Mutat. 2012;33(4):609-613.

4. Lemonnier F, Dupuis J, Sujobert P, et al. Treatment with 5-azacytidine induces a sustained response in patients with angioimmunoblastic T-cell lymphoma. Blood. 2018;132(21):2305-2309.